From RHIC to the EIC

The legacy of RHIC and its connection to the EIC

Lijuan Ruan (BNL)

July 11-12, 2026

@BrookhavenLab

Relativistic Heavy Ion Collider

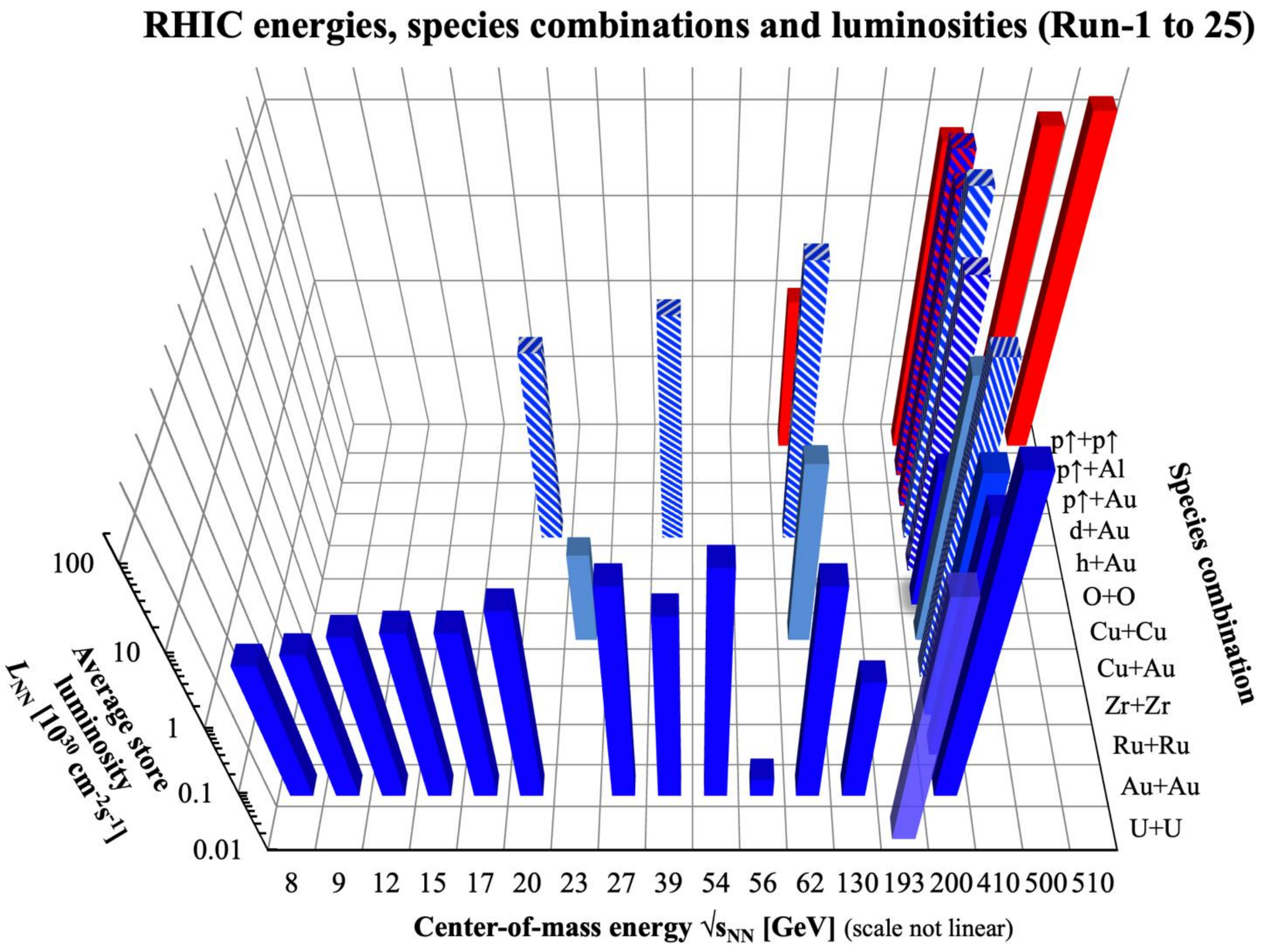

26 years of RHIC operations—the most versatile collider ever built

5 heavy ion experiments: STAR, PHENIX, PHOBOS, BRAHMS, and sPHENIX

The legacy of RHIC

- People and expertise
- Detector and accelerator technologies
- Scientific impact and broader significance

Courtesy of C. Shen

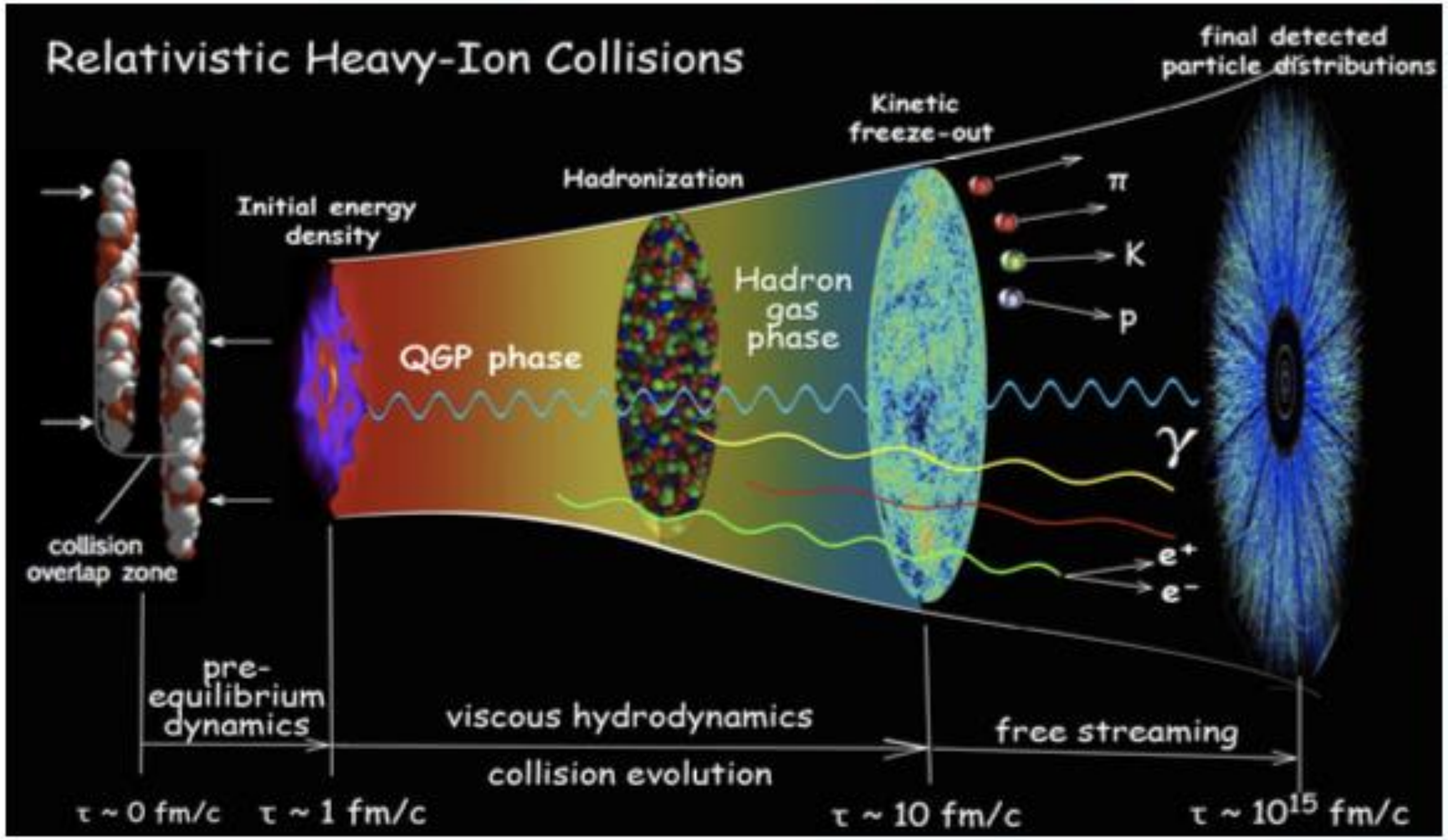

The discovery of perfect liquid

- Hydrodynamic models successfully describe particle spectra and azimuthal anisotropy (v_n) measurements at p_T < 2 GeV/c; statistical hadronization models reproduce particle yields and yield ratios.
- Significant jet quenching effects at high p_T.
- A characteristic baryon-to-meson enhancement pattern at intermediate p_T.

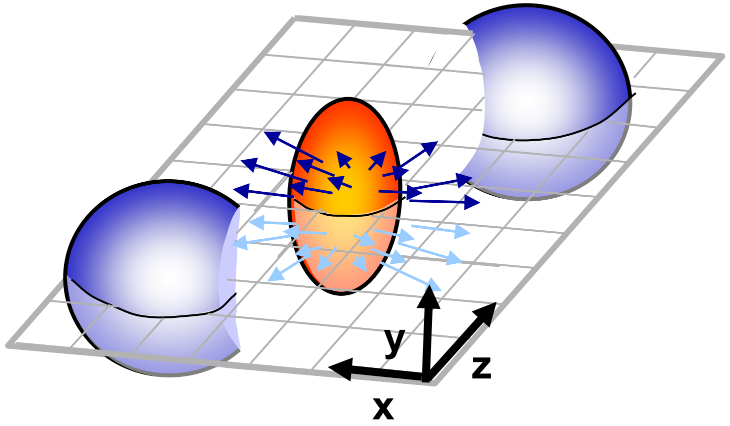

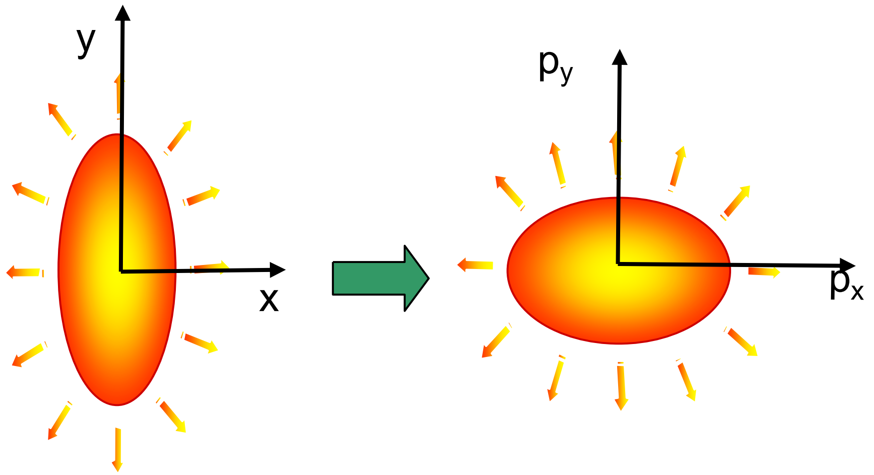

Non-central collisions: azimuthal anisotropy in coordinate-space

Interactions ➔ asymmetry in momentum-space

Sensitive to early time in the system's evolution

Measurement: Fourier expansion of the azimuthal p_T distribution

$$E\frac{d^3N}{d^3p} = \frac{1}{\pi} d^2 \frac{N}{dp_T^2 dy}\left[1 + 2v_1\cos(\varphi - \Psi_R) + 2v_2(2[\varphi - \Psi_R]) + \ldots\right] \Rightarrow v_2 = \langle \cos(2[\varphi - \Psi_R]) \rangle$$

The science of RHIC

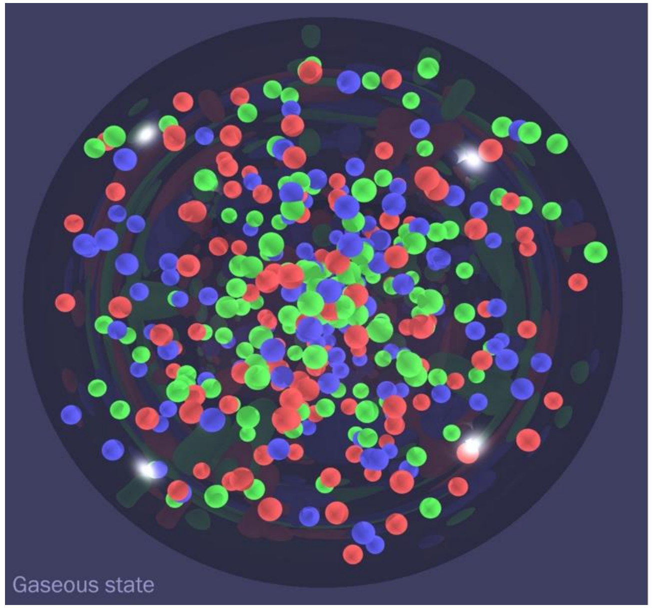

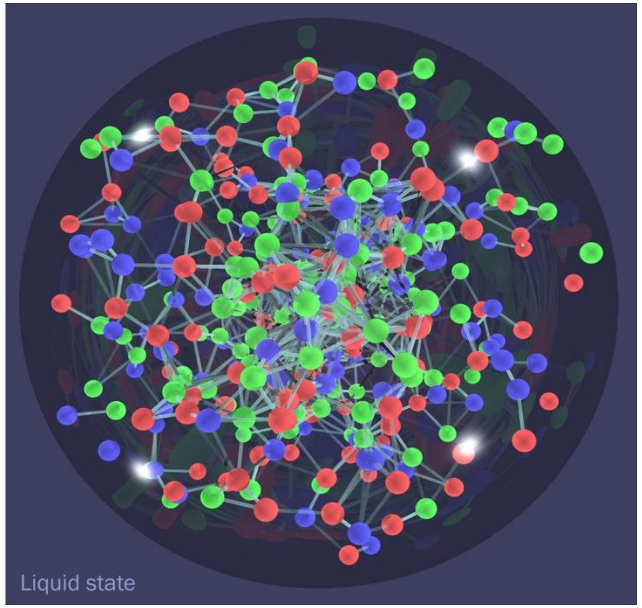

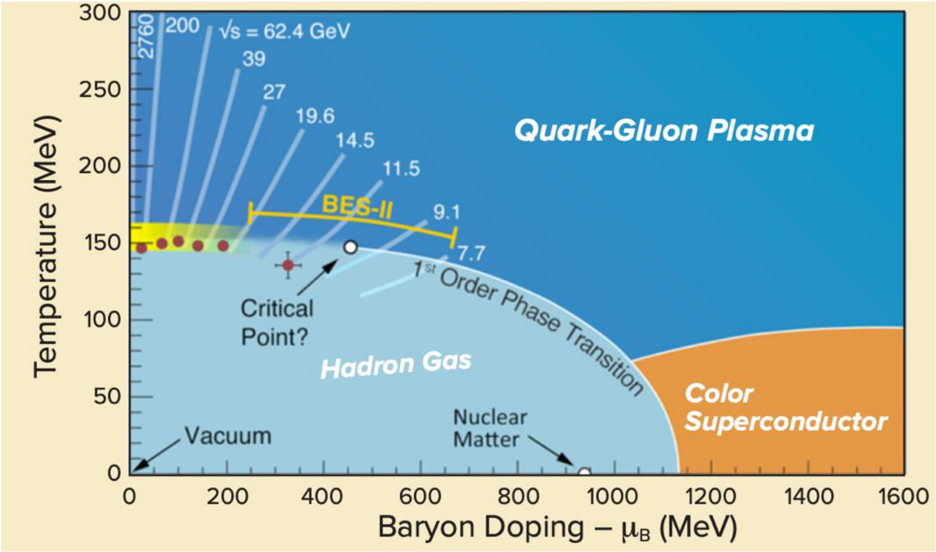

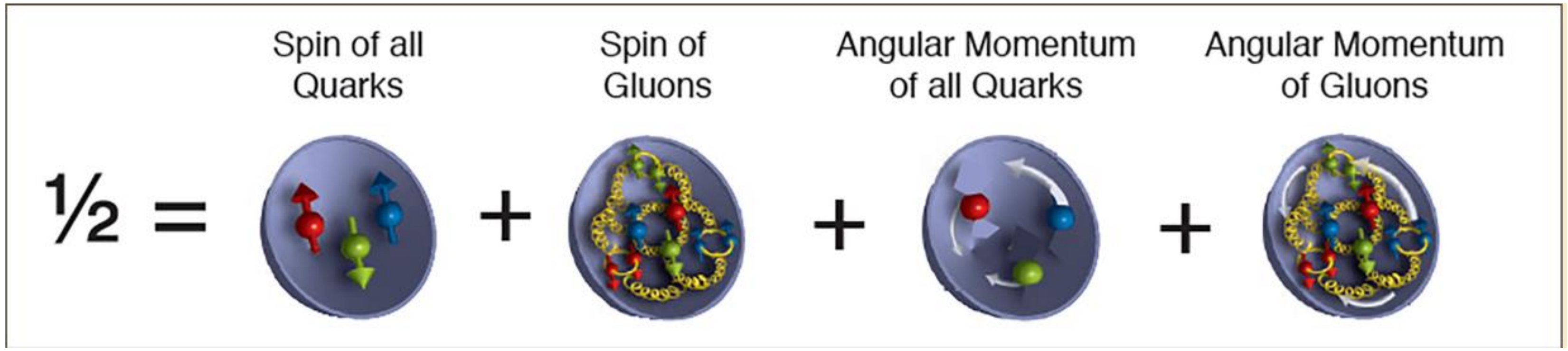

To probe the inner workings of the Quark-Gluon Plasma

To map the phase diagram of QCD

To study the spin puzzle of proton

The properties of perfect liquid

The 2023 NSAC Long Range Plan for Nuclear Science

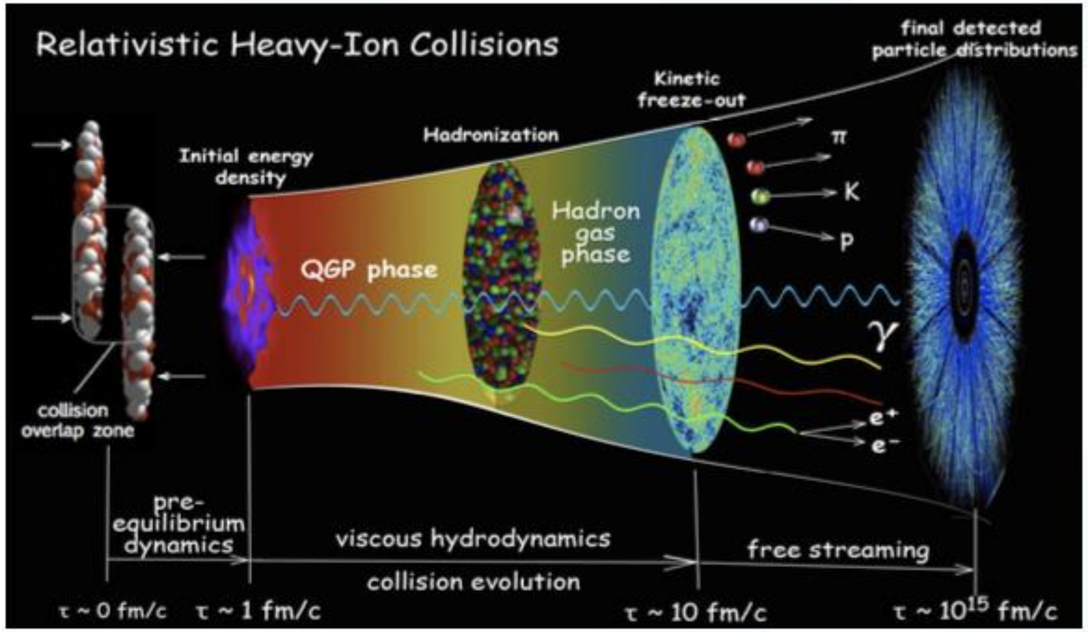

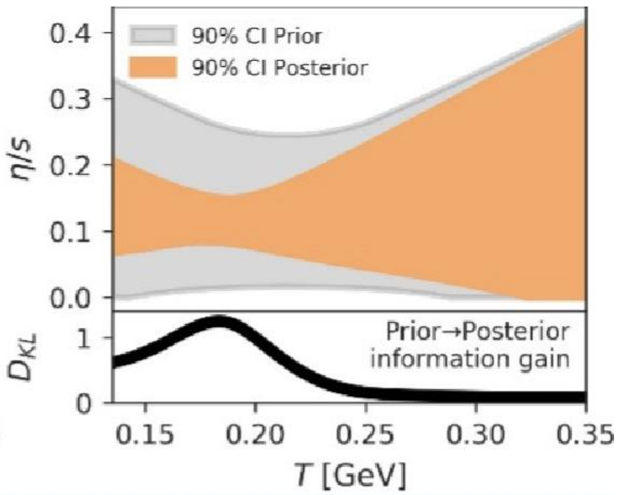

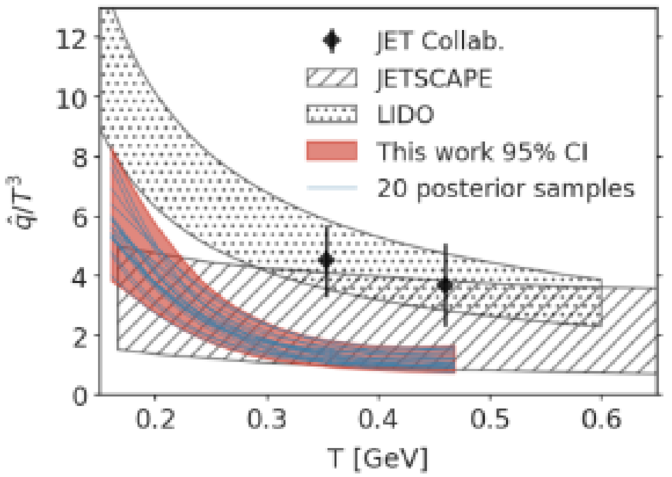

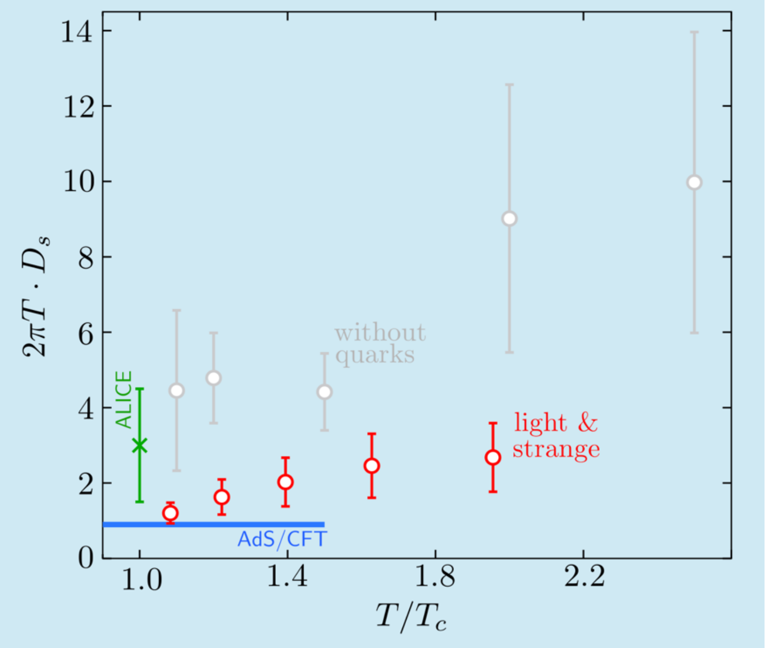

Essential questions to be addressed:

1. How do the fundamental interactions between quarks and gluons lead to the perfect fluid behavior of the quark-gluon plasma?
2. What are the limits on the fluid behavior of matter?
3. What are the properties of QCD matter?
4. What is the nature of the transition from QGP to hadronic matter?
5. Does a QCD critical point exist, analogous to the critical point in the water–vapor–ice phase diagram?

The phases of QCD matter

Lattice QCD: crossover chiral transition at μ_B **< 3 T**

At top RHIC and LHC energies, measurements consistent with a smooth crossover chiral transition

Change T and μ_B by varying the collision energy:
- Search for the critical point
- Search for the first-order phase transition
- Search for the threshold of QGP formation

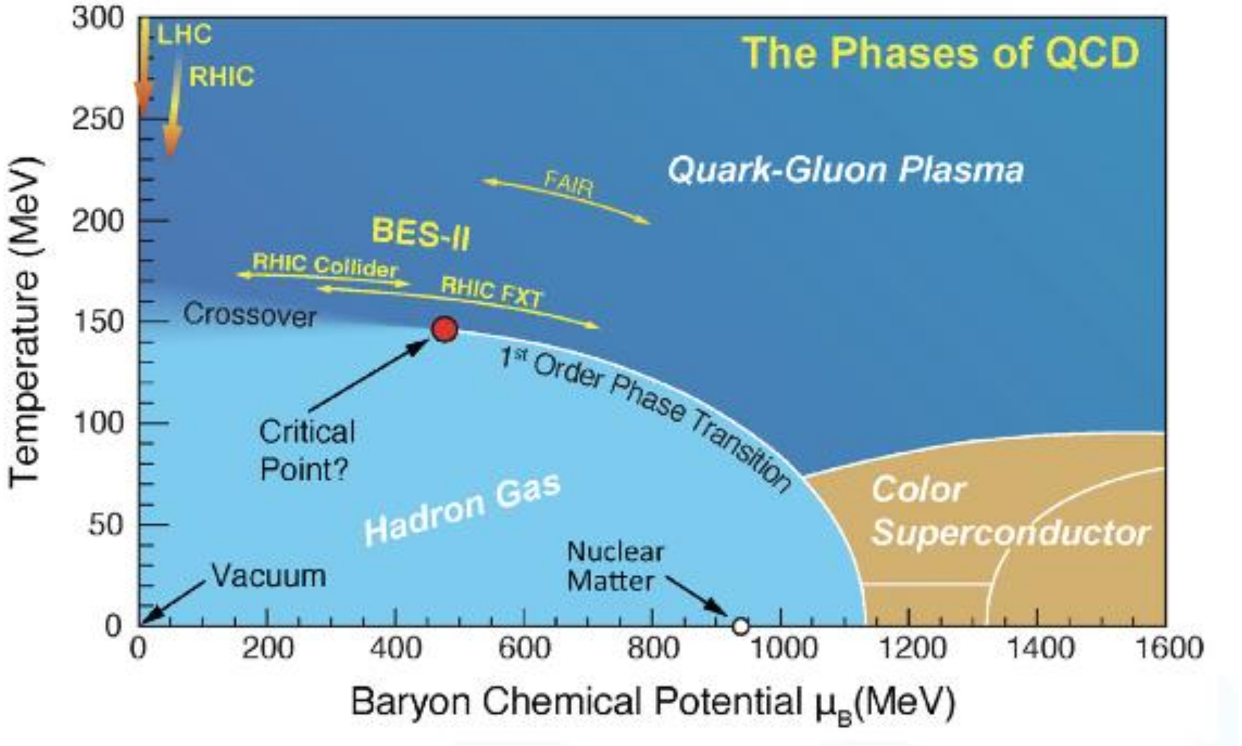

Beam Energy Scan results

With BES-I and BES-II data (including spectra, v_n , correlations and fluctuations, thermal radiation, global polarization, and spin alignment, …), we observe:

- Signatures of QGP turn-off (v_n)
- Non-monotonic behavior in fluctuations (net-proton, mean p_T)
- An intriguing energy dependence of the baryon/meson v_1 slope
- A smooth energy dependence of thermal dilepton production
- Abundant hypernuclei production
- Large global polarization
- …

These results call for a comprehensive, global analysis of all observables, especially with additional data collected in 2026.

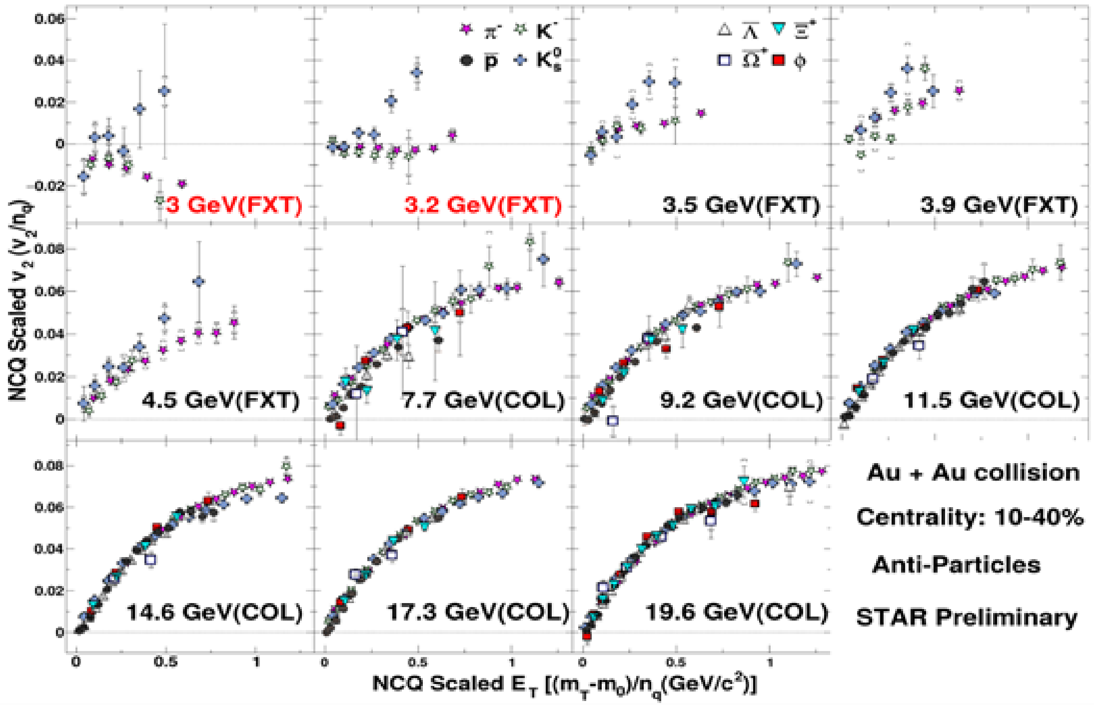

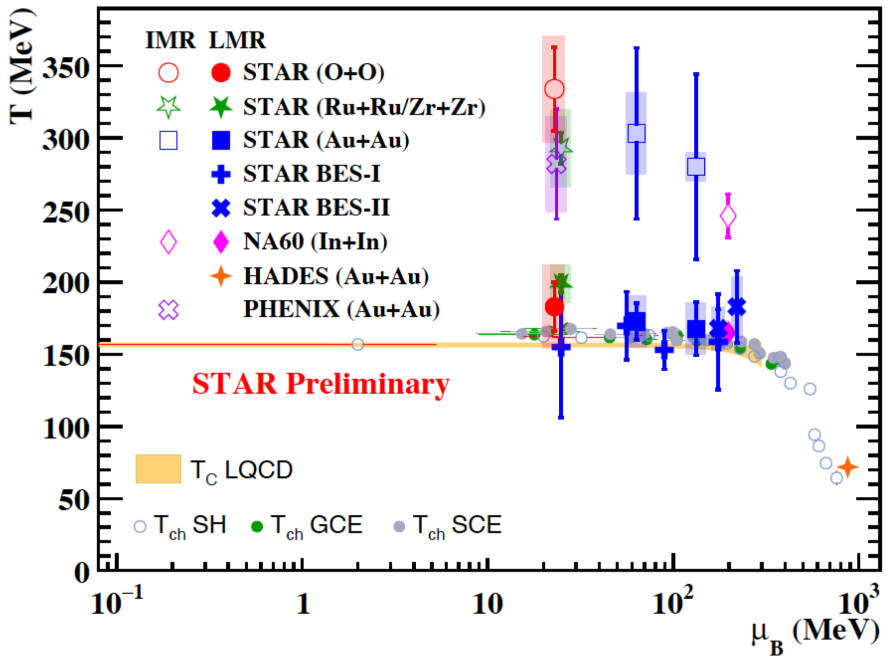

Beam Energy Scan results: fluctuations

STAR, QM2025, PRL**135**(2025)142301

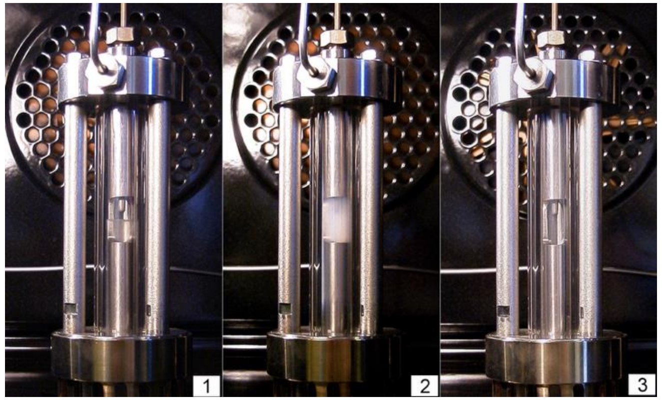

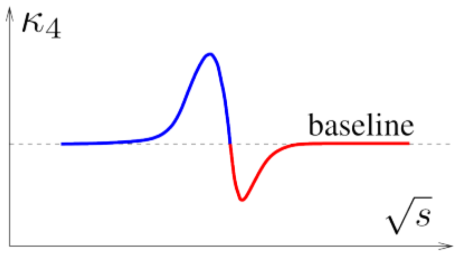

Net-proton

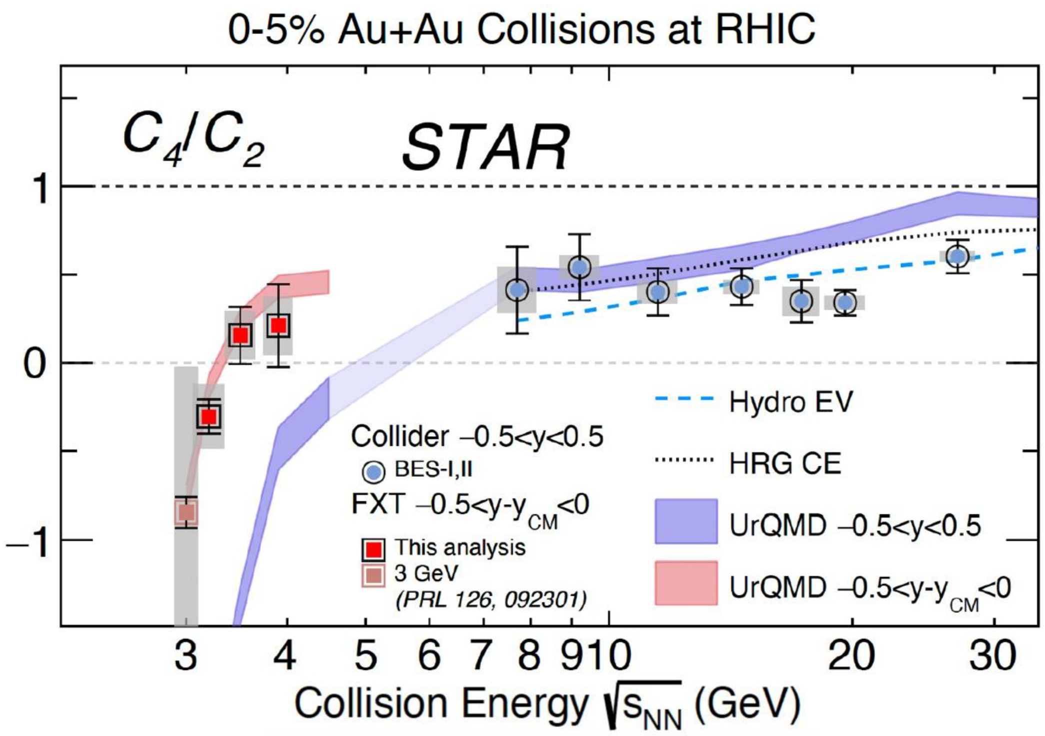

STAR, arXiv: 2604.06434, accepted by PRL

Mean p_T

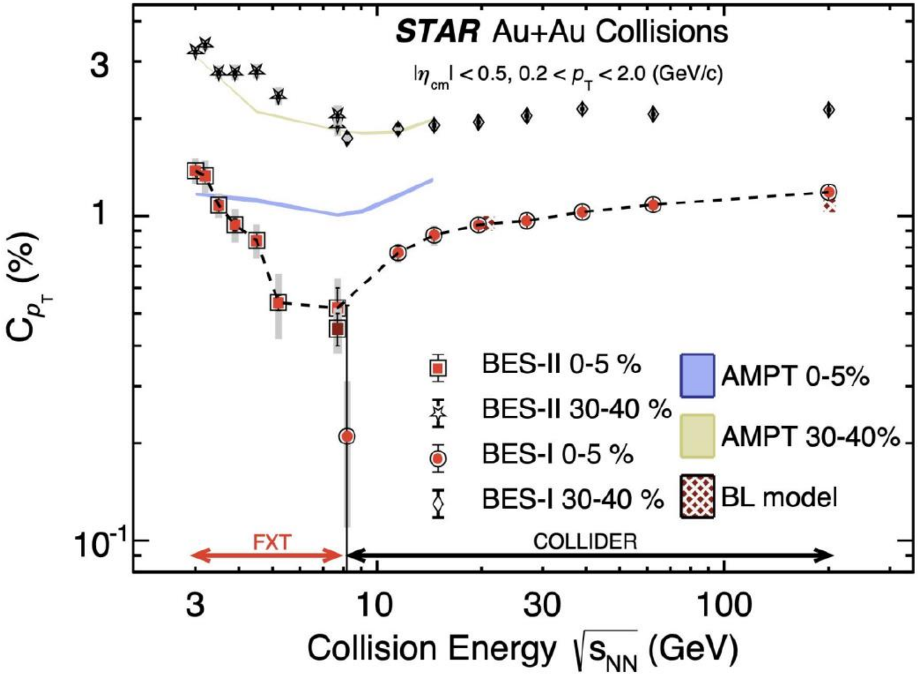

The proton spin

Non-zero gluon spin contribution to the spin of the proton

Advances in transverse spin physics: large transverse single-spin asymmetries at forward rapidity, studies of the Sivers effect and Collins effects, constraints of TMD distributions and spin-orbit correlations.

Constraints of polarized $\Delta\bar{u}$ and $\Delta\bar{d}$

…

Courtesy of C. Gagliardi

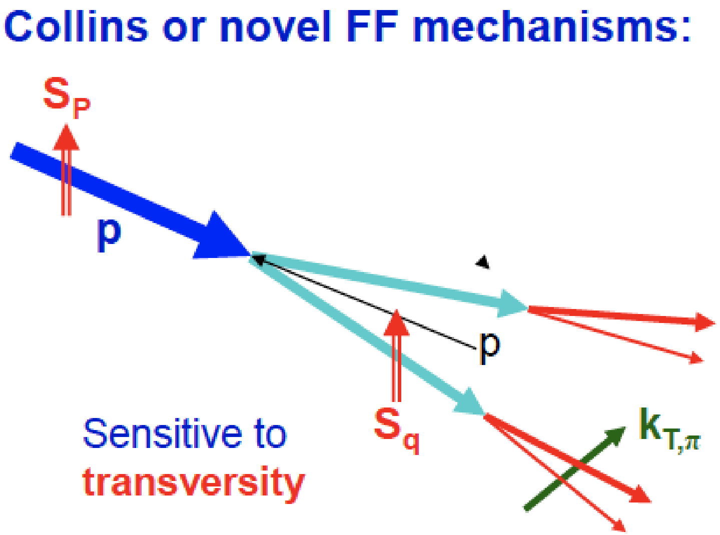

The 2023 NSAC Long Range Plan for Nuclear Science

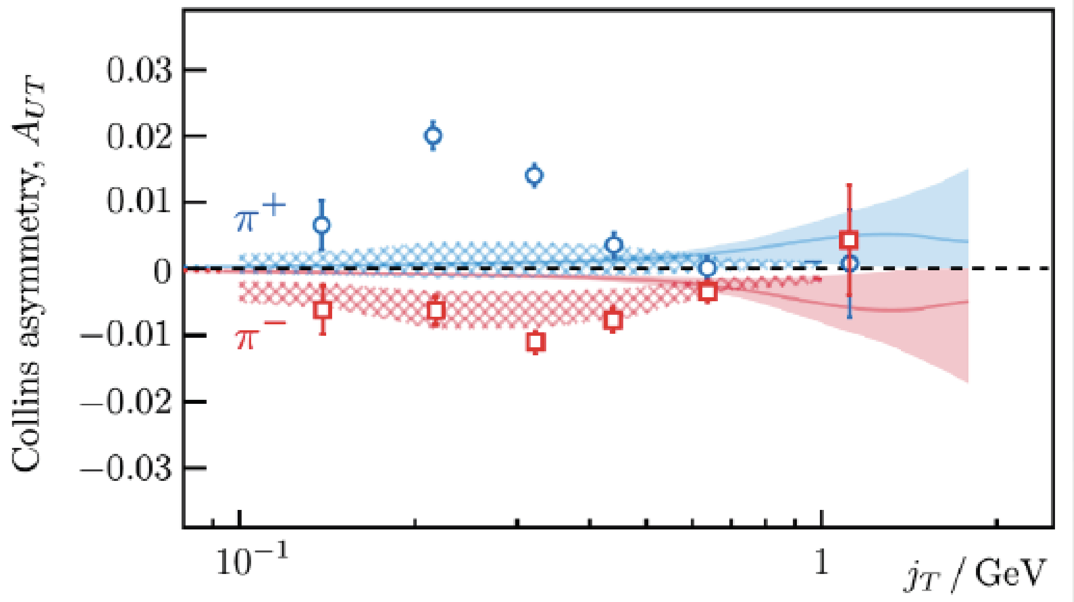

Figure 3.5. Measurements by the STAR experiment at RHIC of the Collins asymmetries for positive and negative pion production in transversely polarized proton-proton collisions. *The Collins TMD distribution describes a spin−momentum correlation in the process of hadronization and is shown here as a function j_T, the momentum of the pion transverse to the jet axis. Theoretical evaluations are shown as bands that do not describe the π^+ data well, indicating the need for improved theoretical understanding [5].*

Broader significance

- Search for the heaviest forms of antimatter
- Strong connections to the nuclear structure community
- Connections to neutron star research
  - Measurements of the QCD equation of state and transport properties can inform our understanding of dense matter in neutron stars and neutron-star mergers.
  - Studies of hypernuclei, including their production, binding energies, and lifetimes, constrain hyperon–nucleon and hyperon–hyperon interactions that may play an important role in the interiors of neutron stars.
- ...

EOS Expanding Horizon White Paper

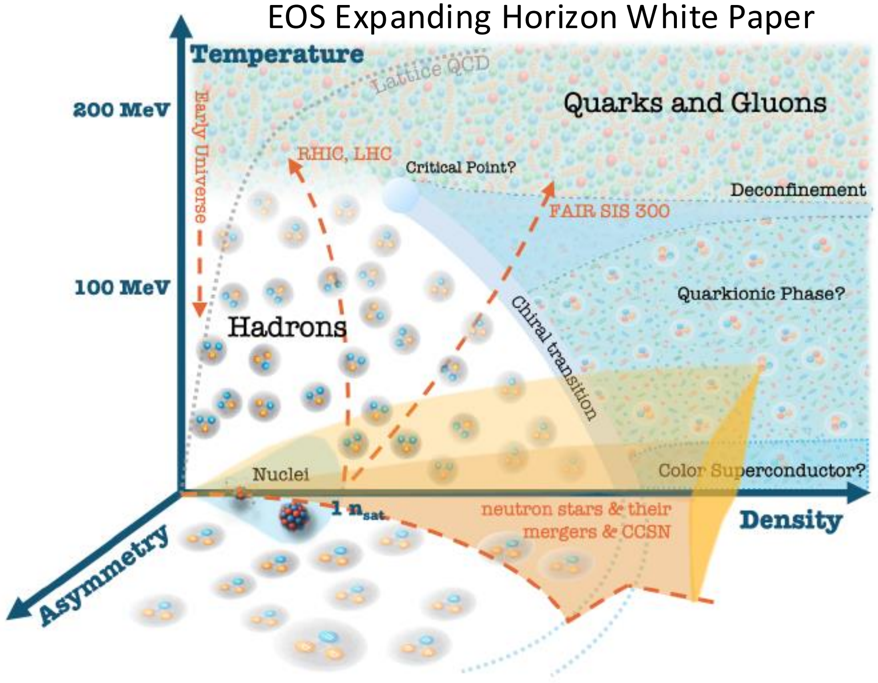

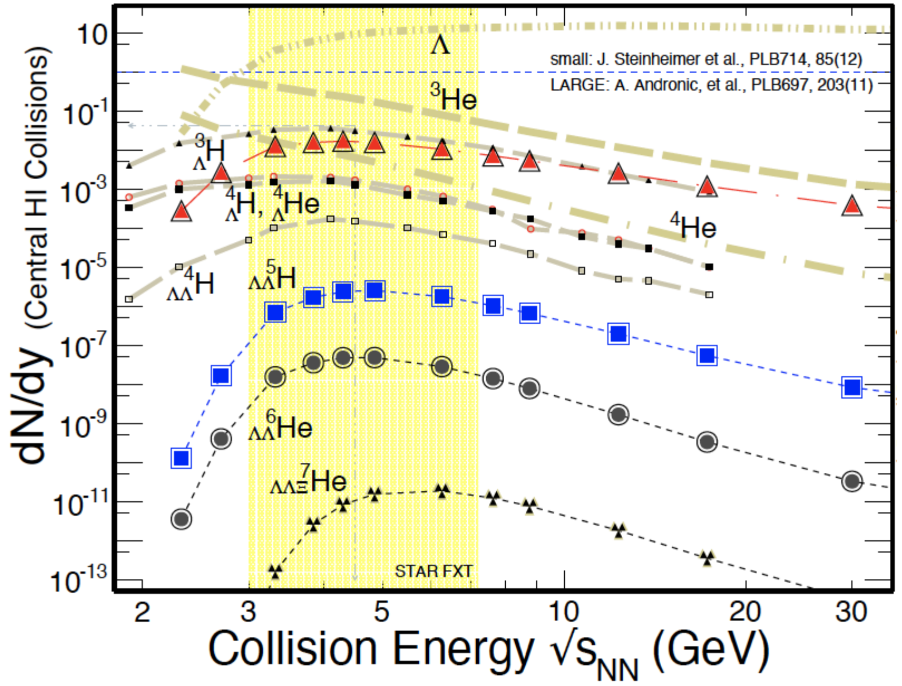

New heaviest exotic antimatter nucleus

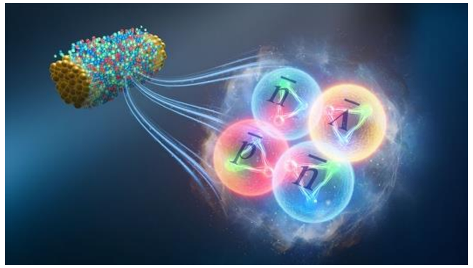

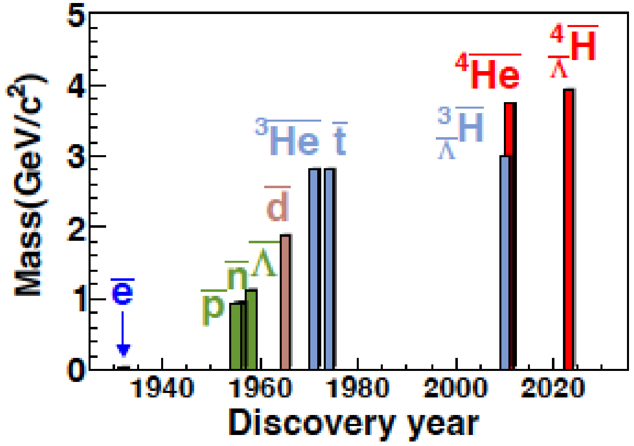

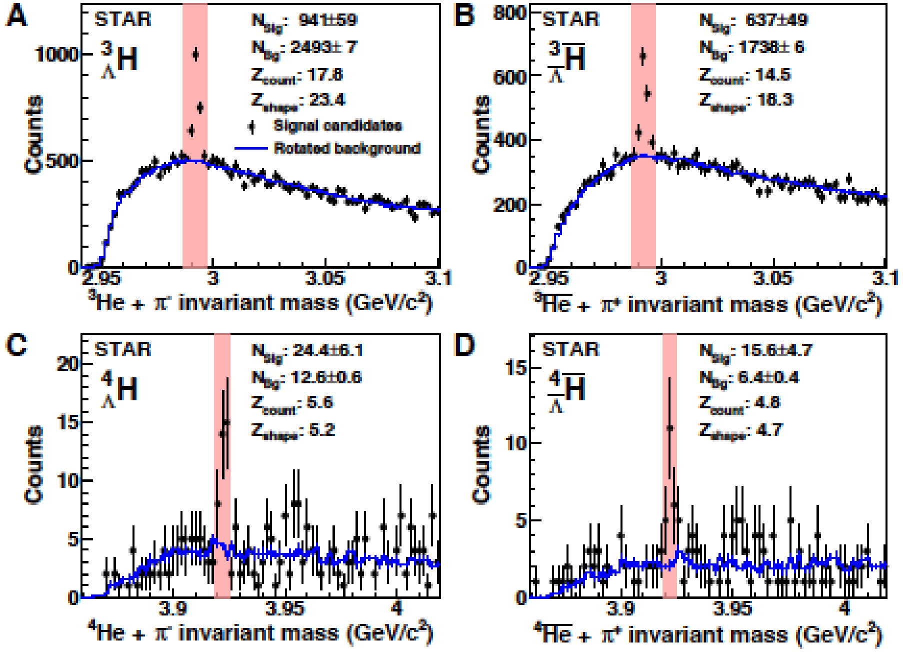

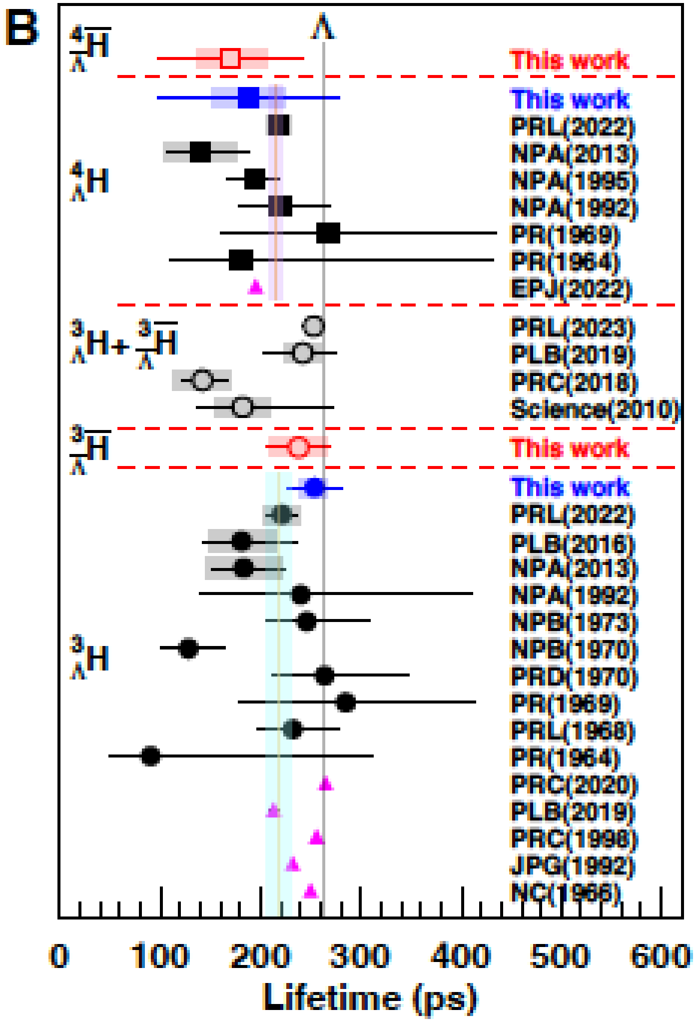

STAR as a discovery machine for antimatter

- First observation of antihyperhydrogen-4

https://www.bnl.gov/newsroom/news.php?a=121912

STAR, Nature 632 (2024) 1026

Imaging shapes of atomic nuclei

https://www.bnl.gov/newsroom/news.php?a=122119
STAR, Nature 635 (2024) 67

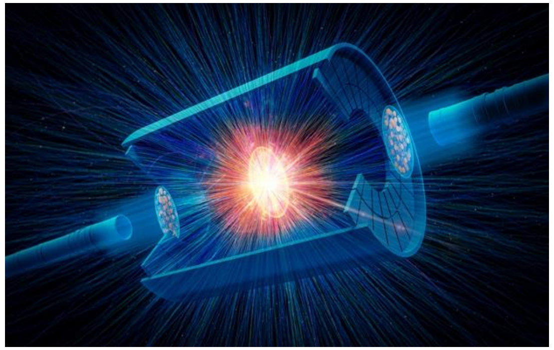

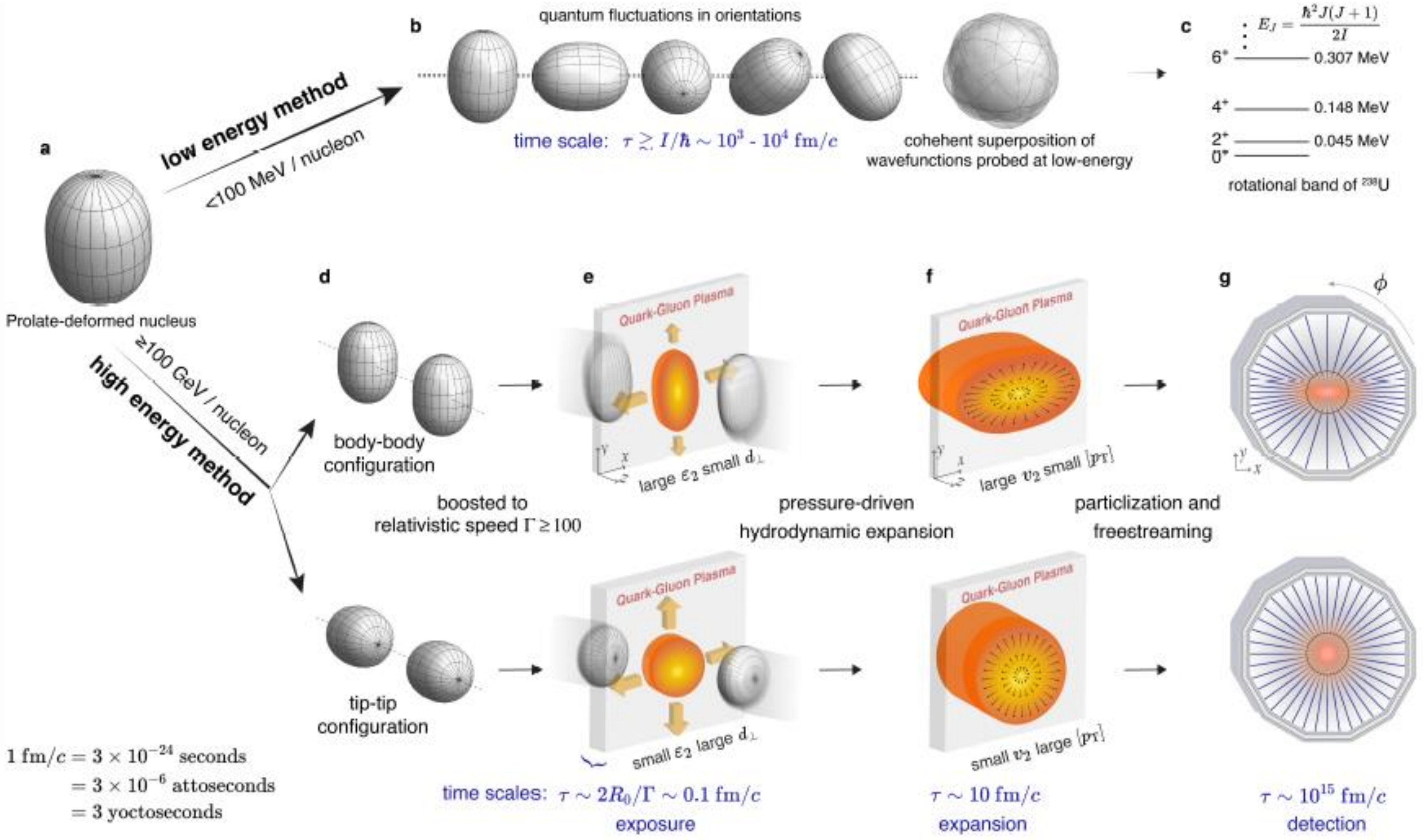

Image the nuclear global shape via colliding them at ultrarelativistic speeds and analyzing the collective response of outgoing debris

The best is yet to come

A. Deshpande, DNP Town Hall, Feb. 13, 2026

STAR Performance 2023-2025

A uniquely versatile experiment at a uniquely versatile collider

Au+Au at $\sqrt{s_{NN}}$=200 GeV (Run 23+24+25) : 16B minimum bias events
- 26.7 nb^{-1} sampled luminosity

pp at $\sqrt{s}$= 200 GeV (Run 24): 164 pb^{-1} sampled luminosity
- 1.5B min. bias events and 1.5B high-mult. events

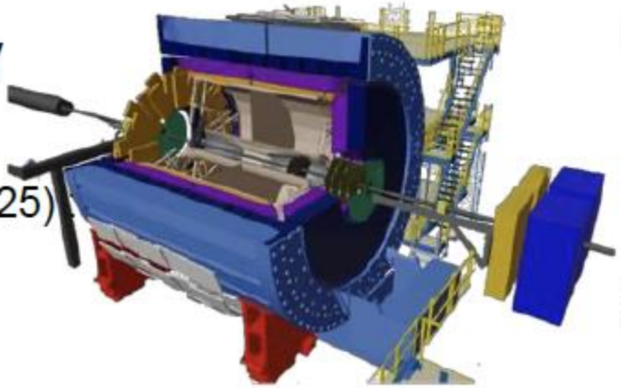

Fixed Target Au+Au at $\sqrt{s_{NN}}$=4.2, 4.5, and 5.2 GeV (Run 25)
- $\sqrt{s_{NN}}$= 4.2 GeV : 290M min.bias events
- $\sqrt{s_{NN}}$ = 4.5 GeV : 1.04B min.bias events
- $\sqrt{s_{NN}}$ = 5.2 GeV : 370M min.bias events

O+O at $\sqrt{s_{NN}}$=200 GeV (Run 25): 136M min.bias, and 269M high-mult. events
- 34 nb^{-1} sampled luminosity

Run 23 AuAu 200

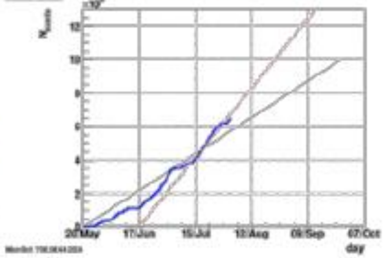

Run 24 AuAu 200

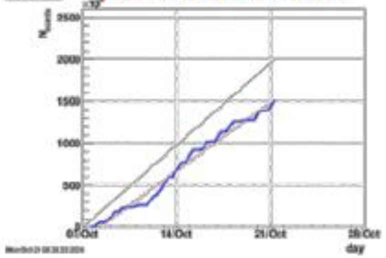

Run25 AuAu 200

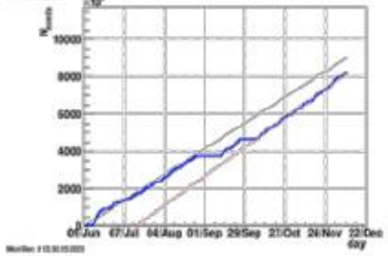

FXT AuAu 4.5

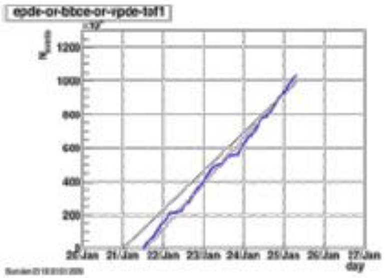

FXT AuAu 4.2

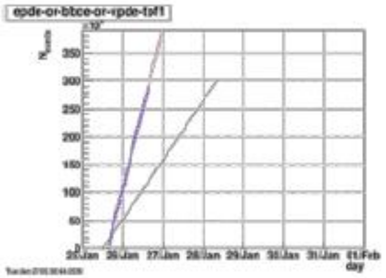

FXT AuAu 5.2

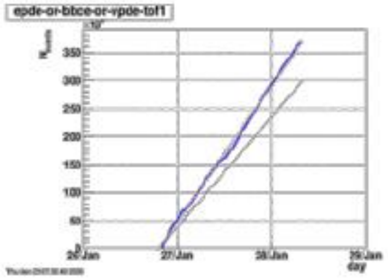

Data Collection: A grand success

Luminosity achieved for triggered all subsystem data

- Au+Au: 6.5/nb, 94% of program goal
  → precision hard probes of QGP
- p↑+p: 30.2/pb, 67% of program goal
  → spin & baseline for QGP studies
- O+O: 23.5/nb, 181% program goal
  → QGP in small system; comparison to LHC

World first spin-polarized streaming collider data: p↑+p: 12.6/pb, 281% program goal

Additionally large calorimeter-only dataset for photon and jet physics in QGP

Overall ~300 Petabyte of experimental data

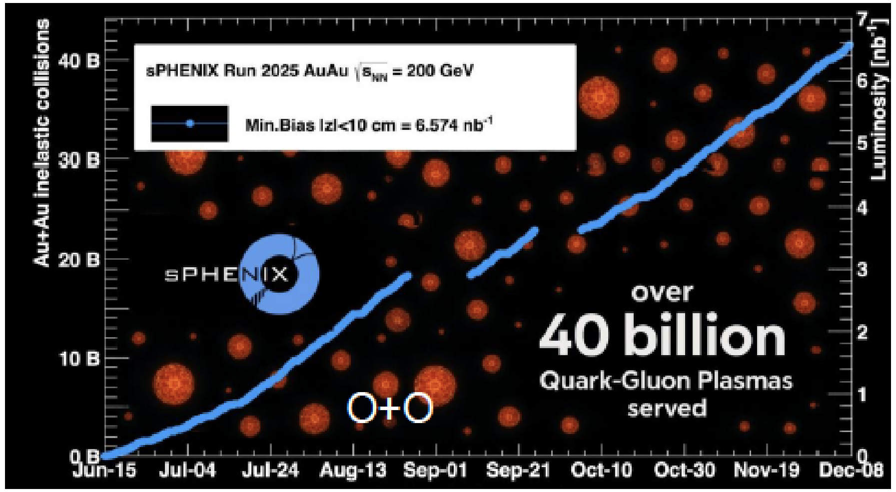

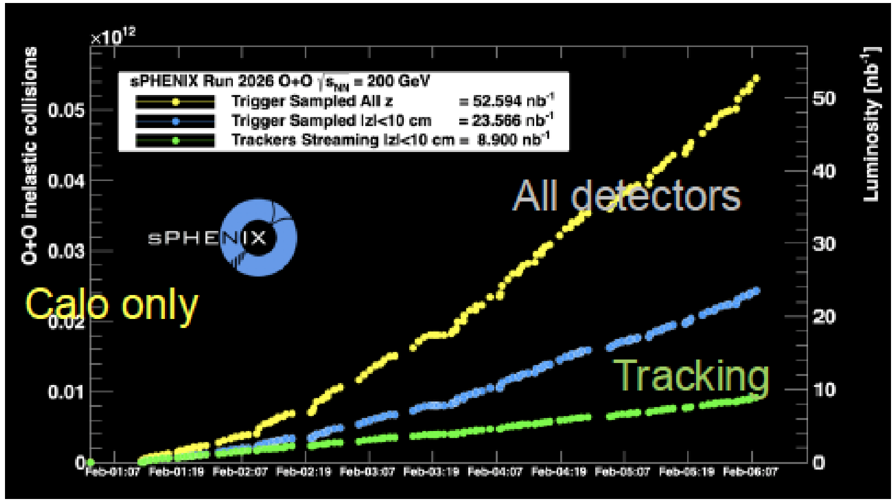

Brookhaven National Laboratory

Connection to the EIC

Emergent phenomena in cold and hot QCD:

- Cold QCD: confinement, mass generation, nucleon and nuclear structure, spin structure of the nucleon …
- Hot QCD: quark-gluon plasma, collective flow, jet quenching, hadronization, and critical phenomena …
- Common themes: many-body quantum dynamics, confinement and hadronization, parton distributions and fragmentation functions, parton shower evolution, spin and orbital motion …

Photon-induced processes: γ–A and γ–γ interactions

(un)Polarized p+p and p+A physics program

…

Photon interactions in A+A

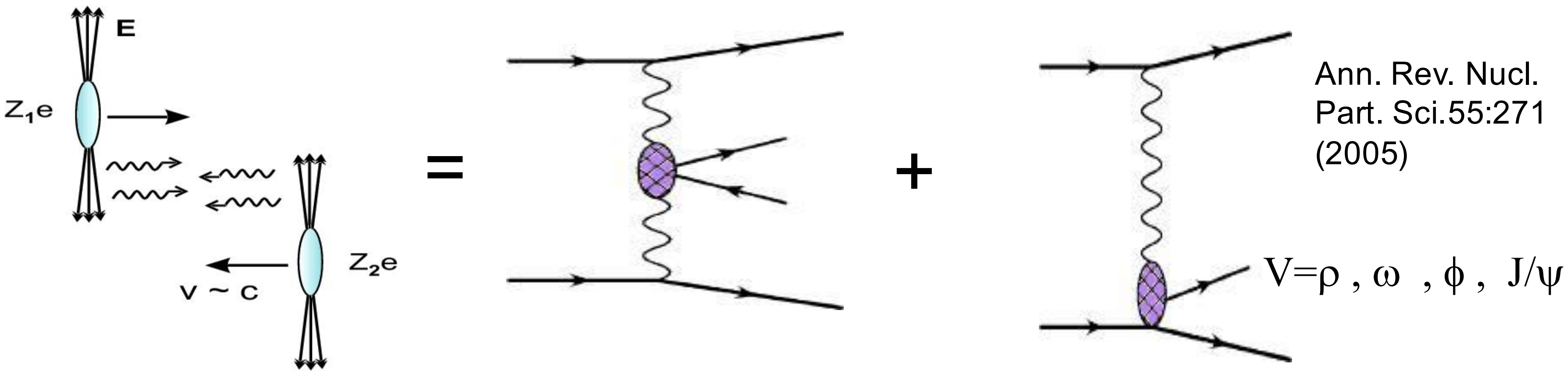

Ann. Rev. Nucl. Part. Sci.55:271 (2005)

Electromagnetic interaction | Photon-photon interactions | Photon-nucleus interactions

- This large flux of quasi-real photons makes a hadron collider also a photon collider
  - ✓ Photon-photon interactions: dileptons …
  - ✓ Photon-nucleus interactions: vector meson
- Conventionally studied in ultra-peripheral collisions (UPC)

Very low p_T J/ψ in heavy ion collisions

ALICE: PRL 116 (2016) 222301

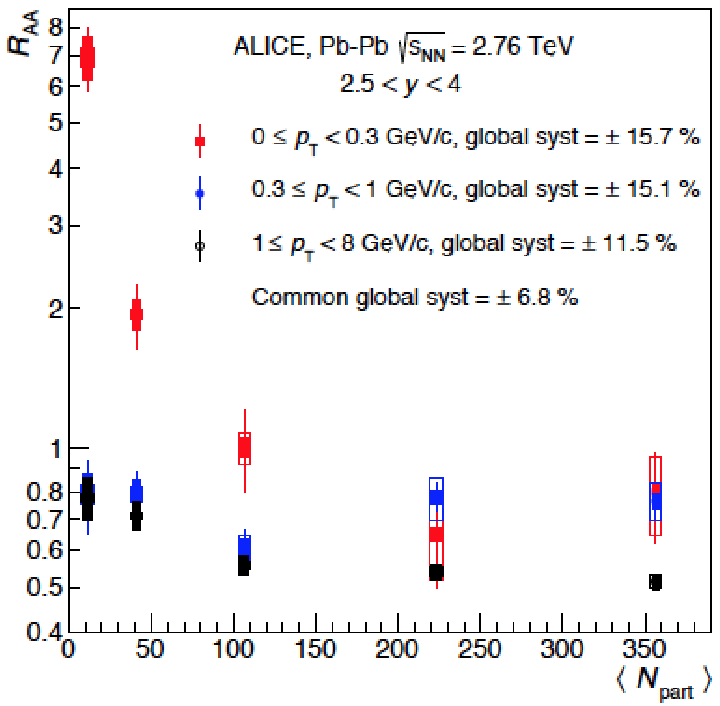

Published later at PRL 123 (2019) 132302 by STAR

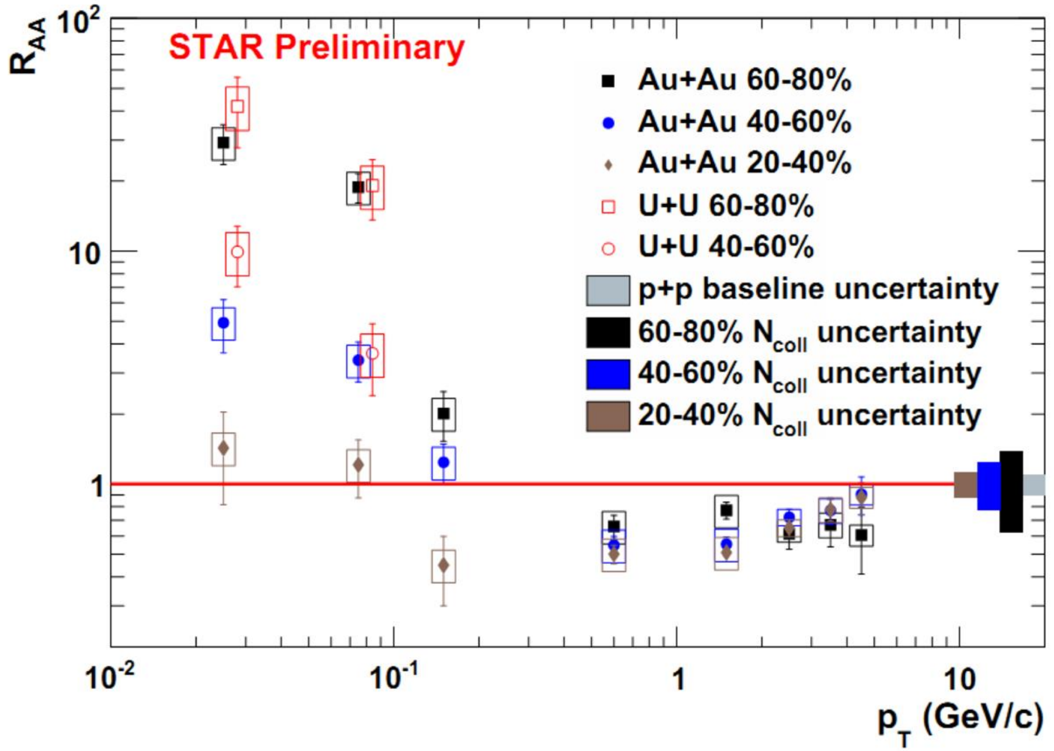

Large enhancement of J/ψ yield observed in peripheral A+A collisions!

Prominent centrality and p_T dependence.

J/psi yield vs. $t=p_T^2$

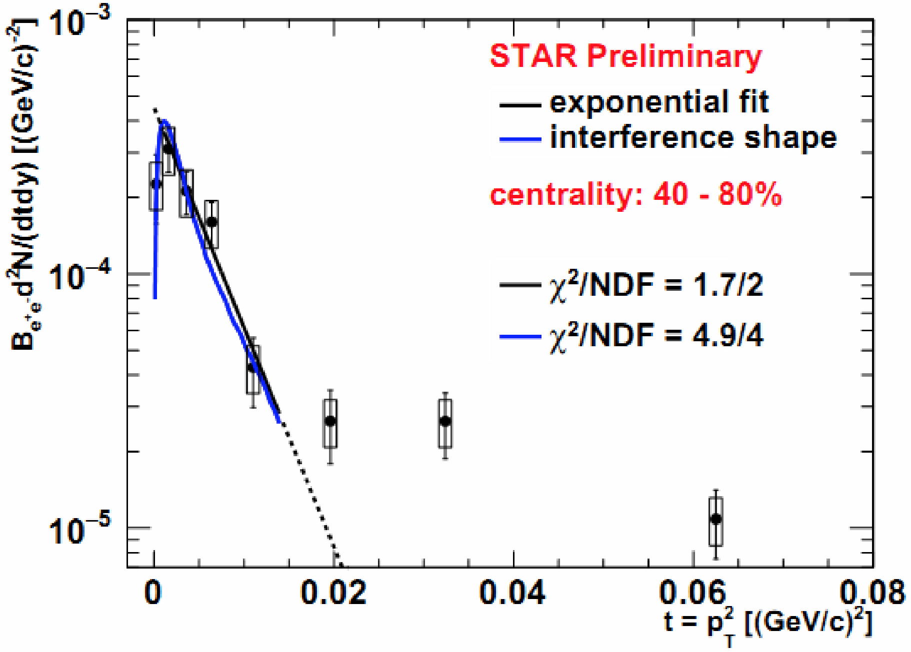

Slope parameter consistent with the size of the Au nucleus. Interference structure observed. Coherent photon-nucleus interactions!

Very low p_T e^+e^- signal

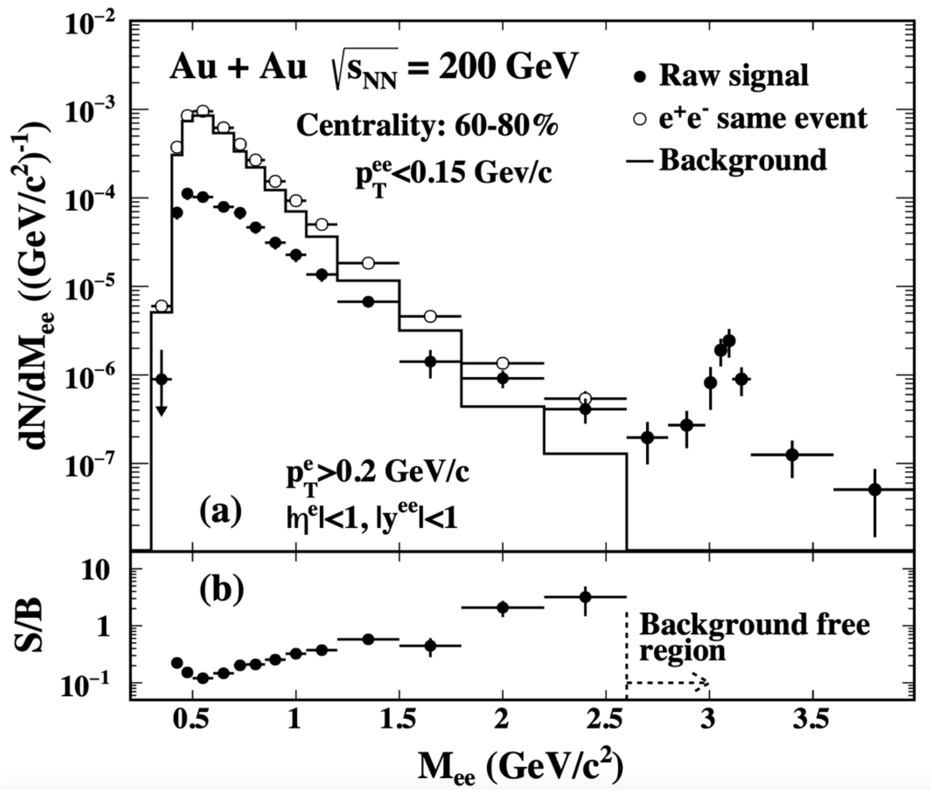

STAR: Phys. Rev. Lett. 121 (2018) 132301

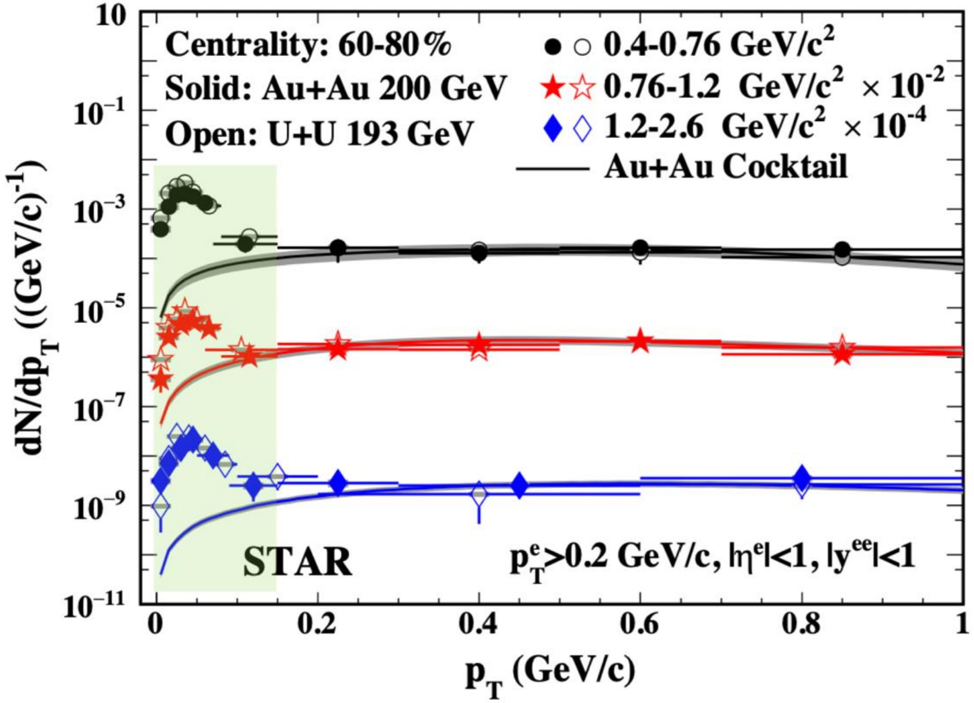

The excess is large at low p_T

Very low p_T e^+e^- signal

STAR: Phys. Rev. Lett. 121 (2018) 132301

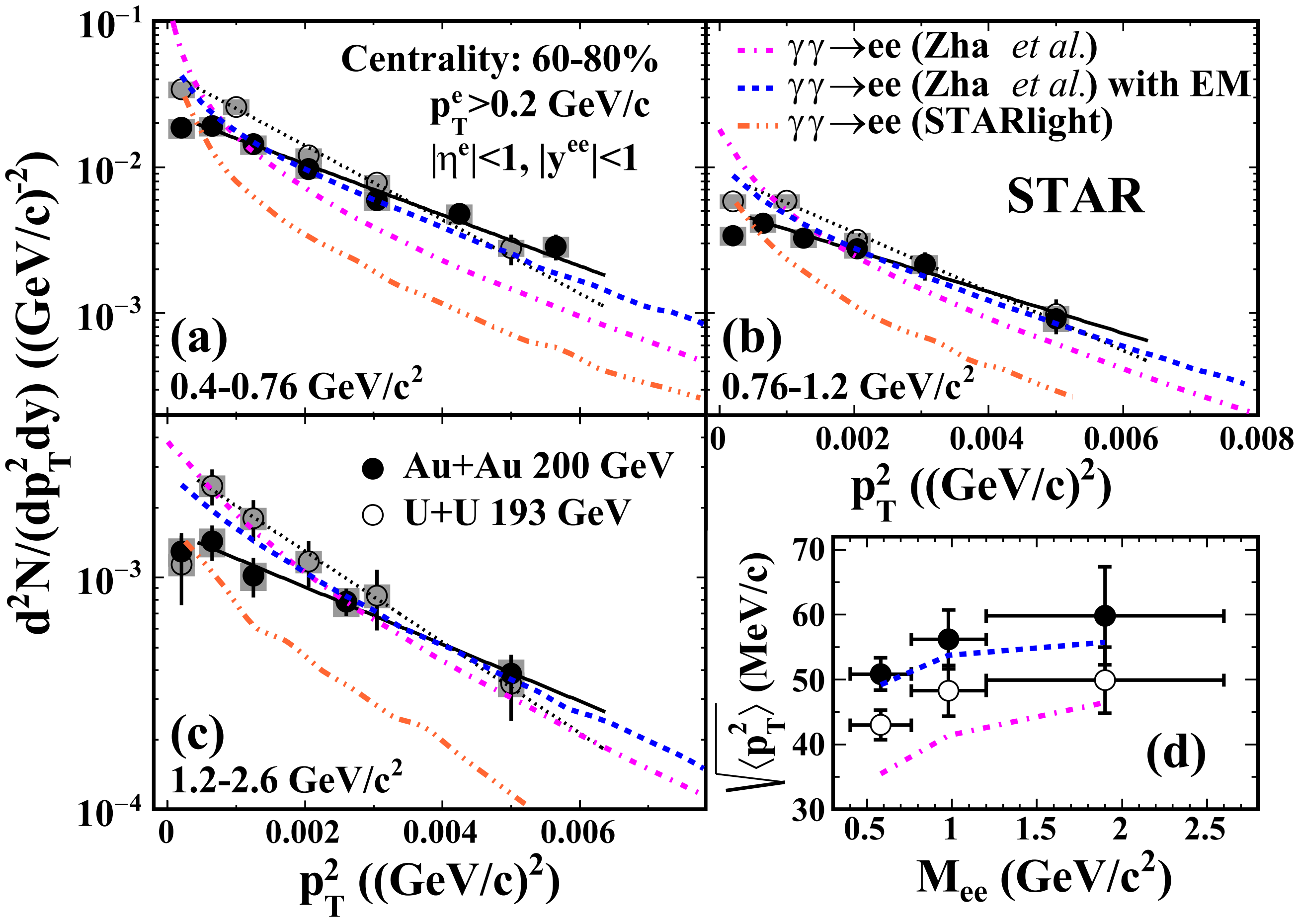

p_T^2 distribution could be sensitive to magnetic field effect (eBL~30 MeV/c, B~10^{14}T, L~ 1fm)

Dimuon acoplanarity

ATLAS: PRL 121 (2018) 212301

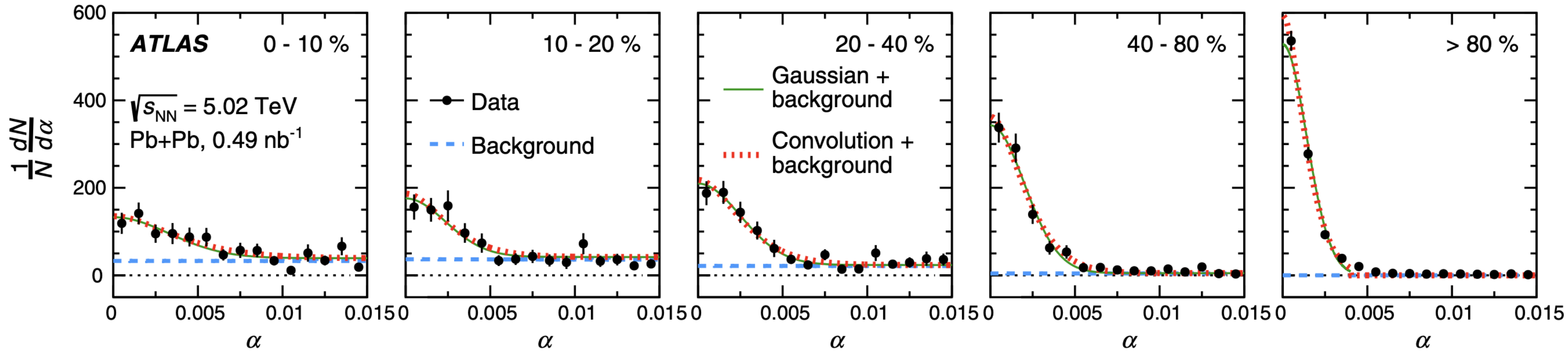

$$\alpha = 1 - \frac{|\phi^+ - \phi^-|}{\pi}, \alpha \propto p_T^{l^+l^-}$$

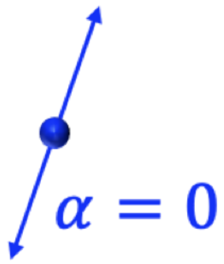

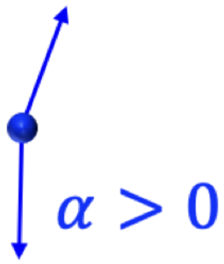

Back-to-back correlation is broadened towards central collisions, could be sensitive to multiple scattering effect

Discoveries of Breit-Wheeler process and vacuum birefringence

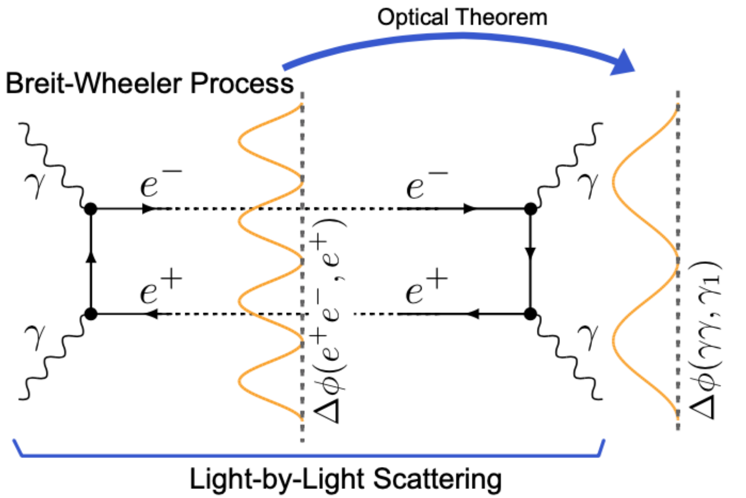

FIG. 1. A Feynman diagram for the exclusive Breit-Wheeler process and the related Light-by-Light scattering process illustrating the unique angular distribution predicted for each process due to the initial photon polarization.

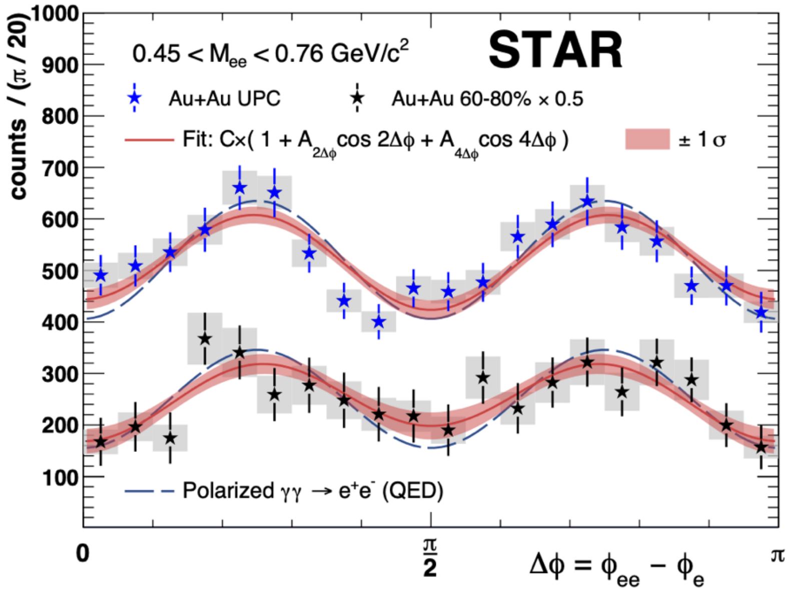

STAR, PRL127 (2021) 52302

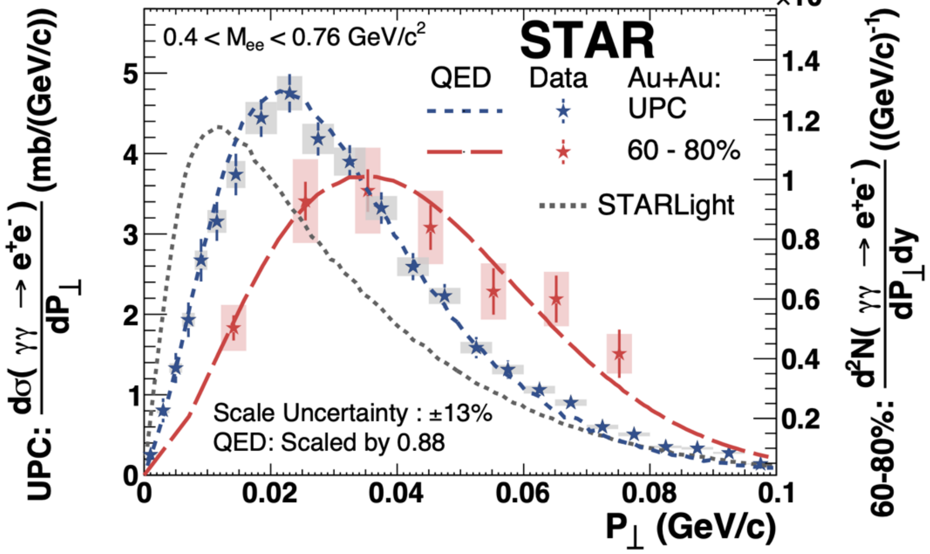

Observation of Breit-Wheeler process with all possible kinematic distributions (yields, M_{ee}, p_T, angle)

Dielectron p_T spectrum: broadened from large to small impact parameters

Observation of vacuum birefringence: 6.7σ in Ultra-peripheral collisions

Collisions of Light Produce Matter/Antimatter from Pure Energy:
https://www.bnl.gov/newsroom/news.php?a=119023

Dimuon acoplanarity in UPC

CMS: Phys. Rev. Lett. 127 (2021) 122001

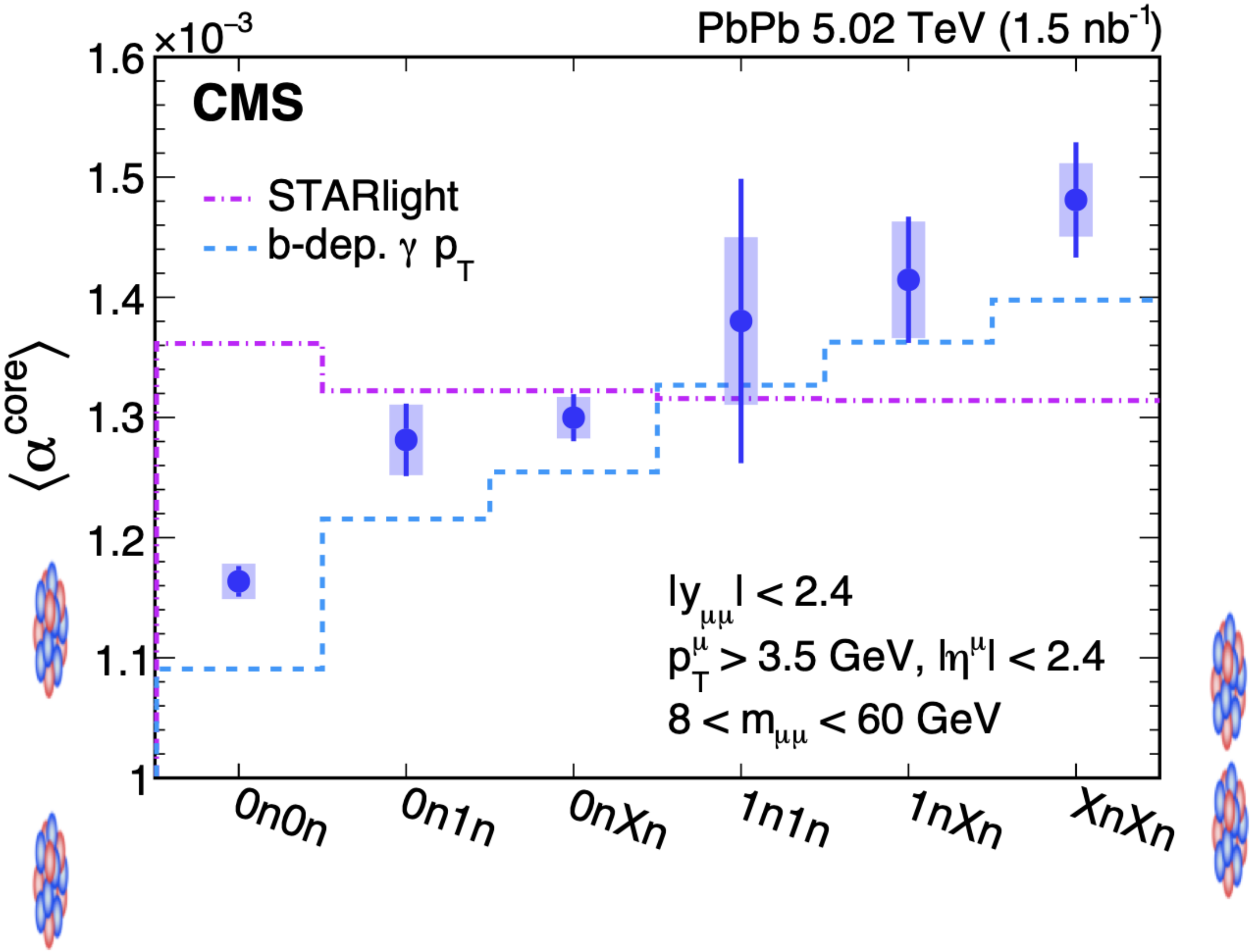

Tomography of ultra-relativistic nuclei with gamma + A collisions

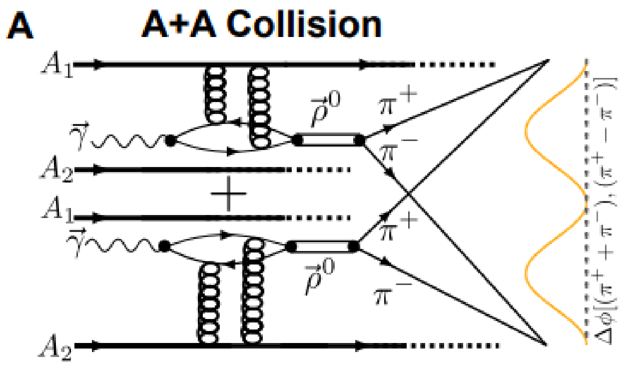

STAR, Science Advances 9 (2023) 3903

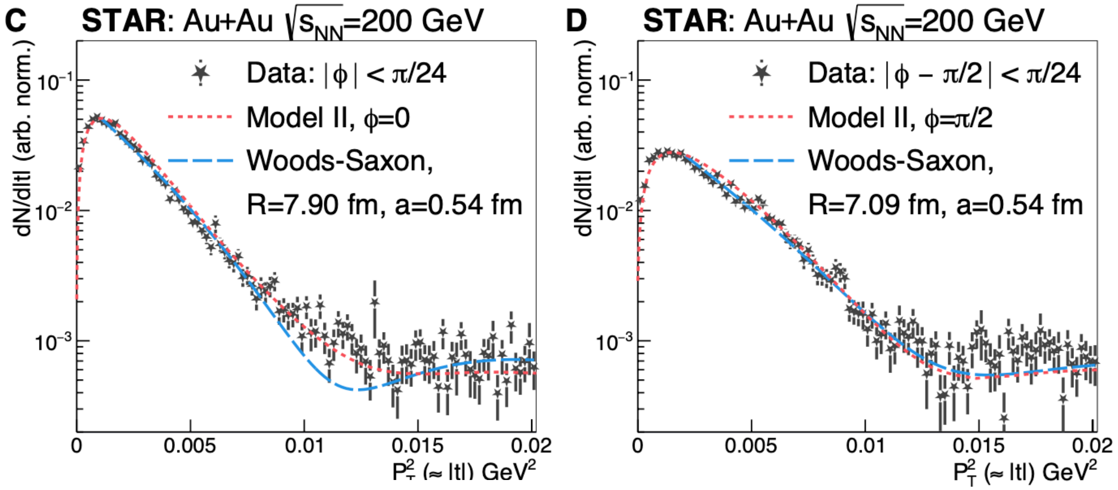

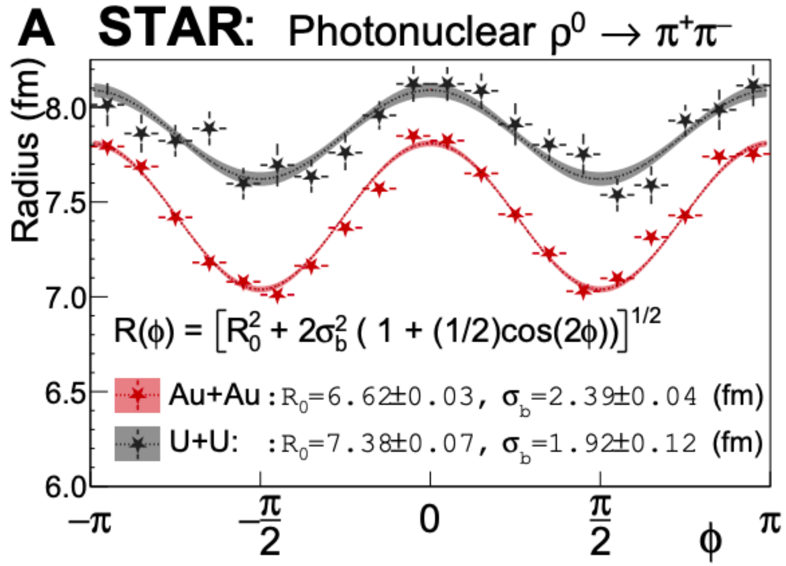

$$\rho_A(r; R, a) = \frac{\rho_0}{1 + \exp[(r - R)/a]},$$

Quantum interference enabled nuclear tomography:

- A novel approach to extract the strong-interaction nuclear radii, which were found to be larger than the nuclear charge radii

Spin interference in photoproduced rho and J/psi

STAR, PRL136 (2026) 242302

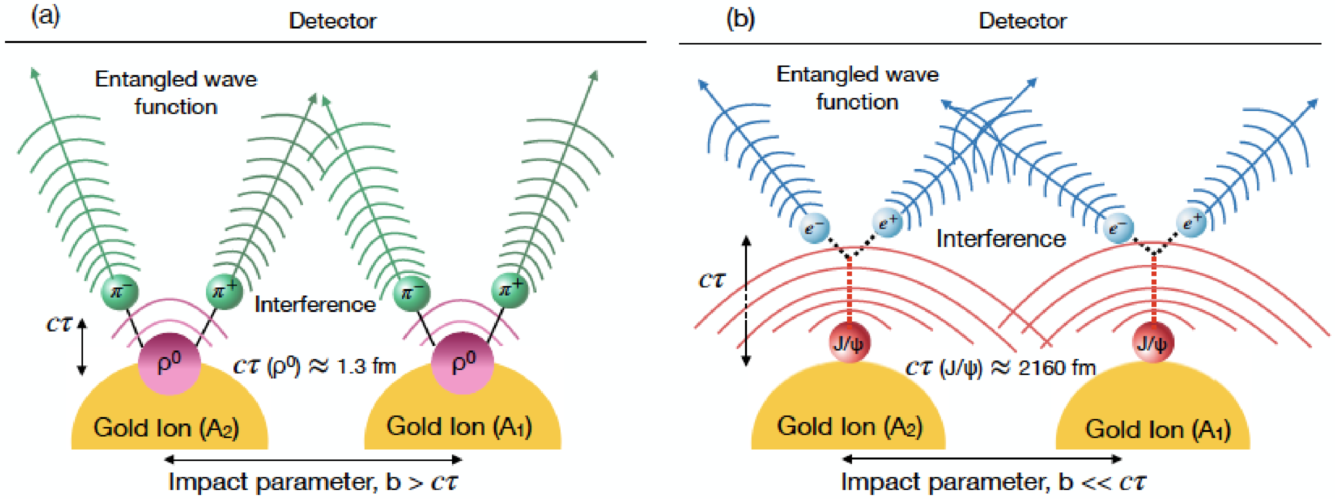

cos(2phi) modulation

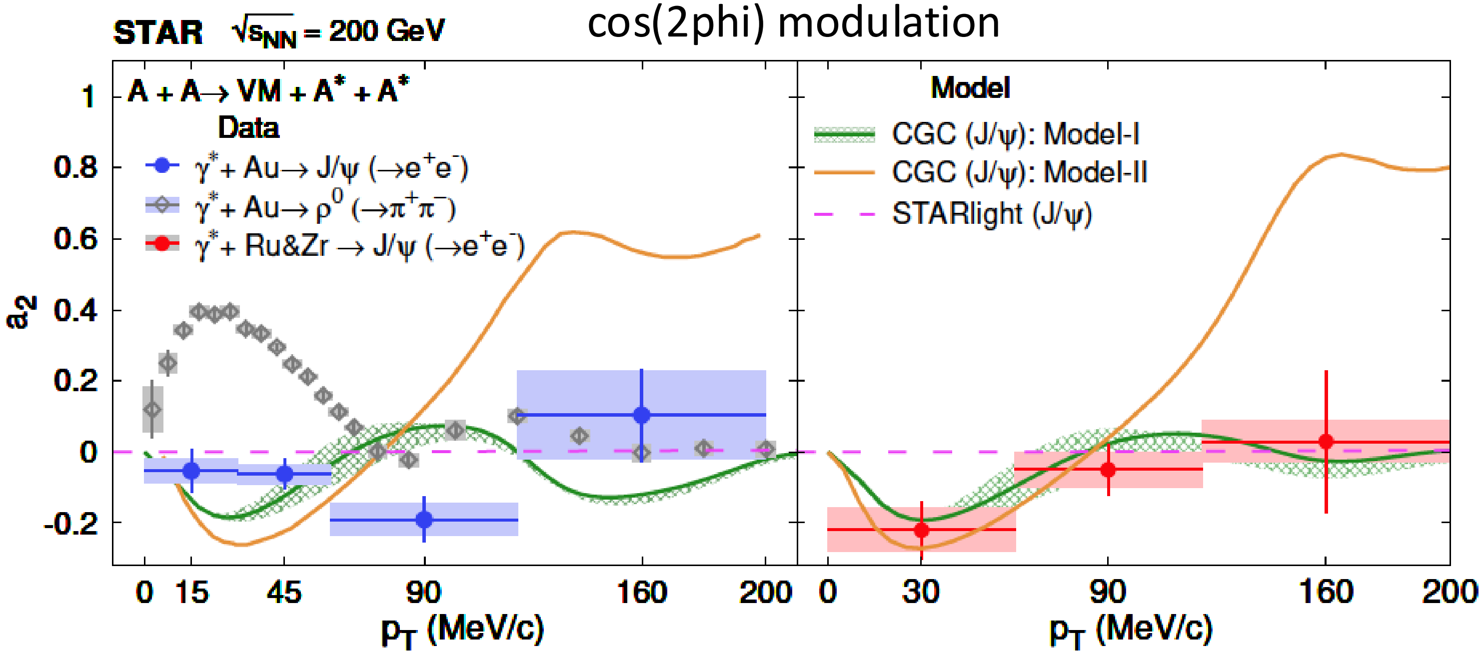

Positive cos(2phi) modulation for rho
Negative cos(2phi) modulation for J/psi

- Interference sign controlled by the spin structure of the final-state daughters
- J/psi probes gluon distributions at perturbative scales: weaker modulations, constraints of the CGC calculations

Coherent and incoherent J/psi photoproduction in UPC

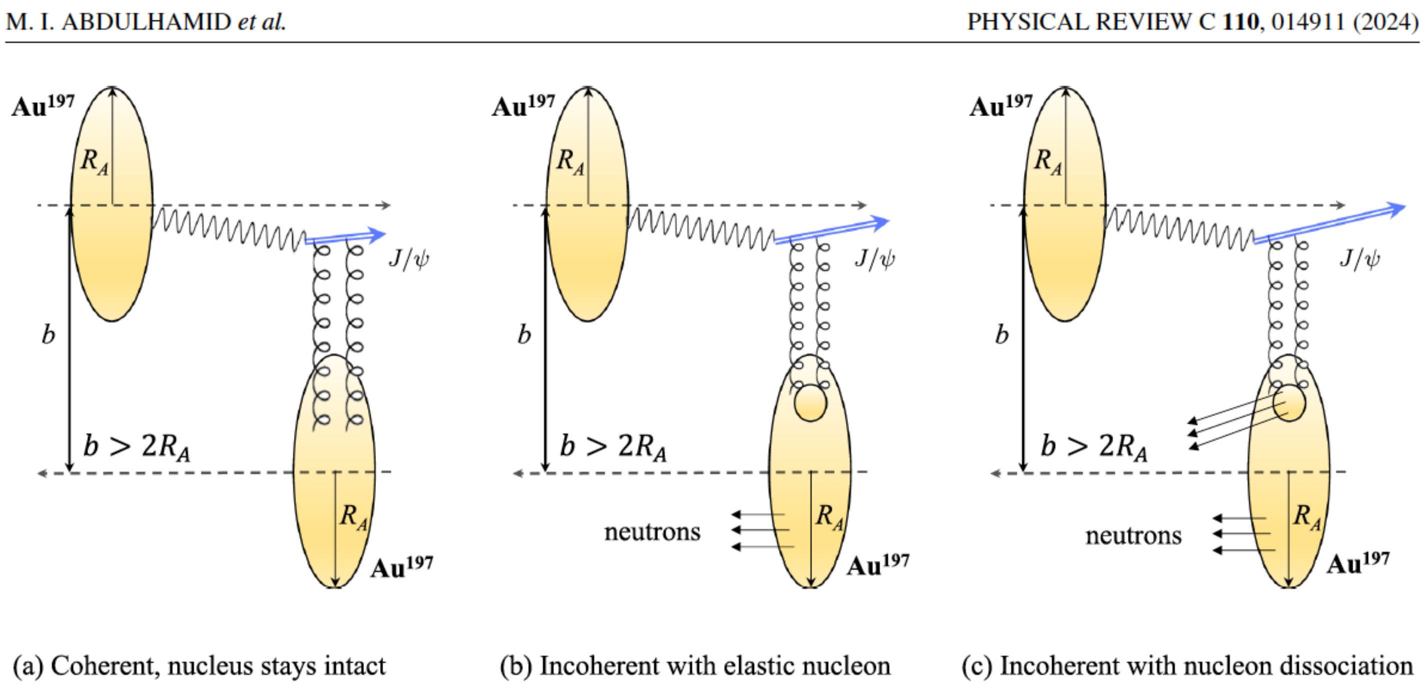

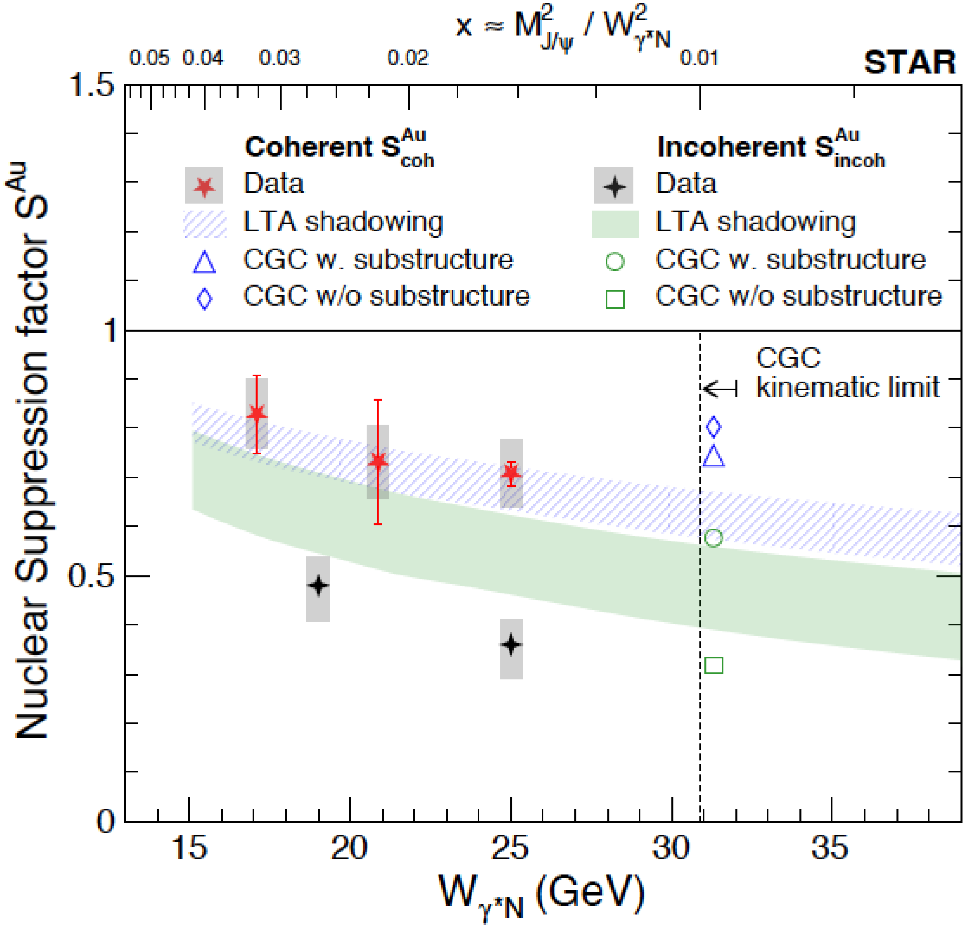

- Incoherent nuclear suppression via J/psi photoproduction, measured **by STAR for the first time**, indicates a stronger modification than its coherent counterpart – a sensitive experimental probe to bound verse free nucleon and its implication to the Cold Nuclear Matter effect.

STAR, Phys. Rev. Lett. 133 (2024) 5, 052301
Phys. Rev. C 110 (2024) 014911

Prospects for e+A collisions

Maci Kesler et al., arXiv: 2502.15596

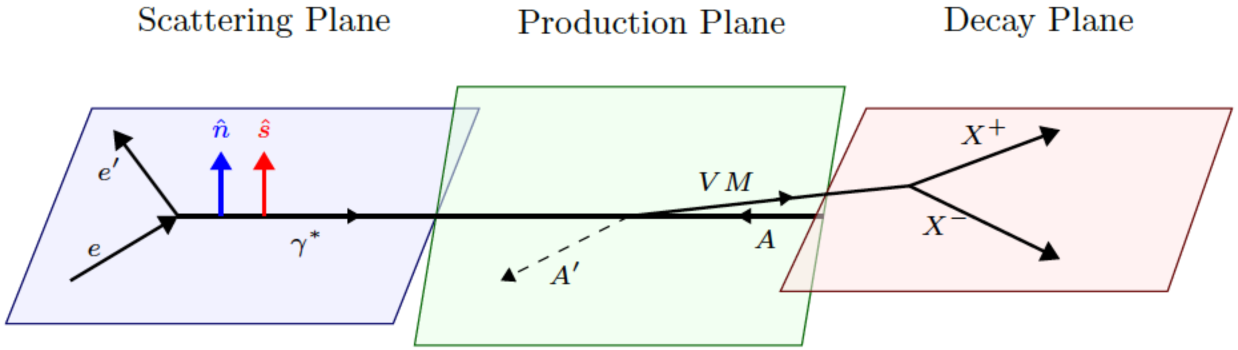

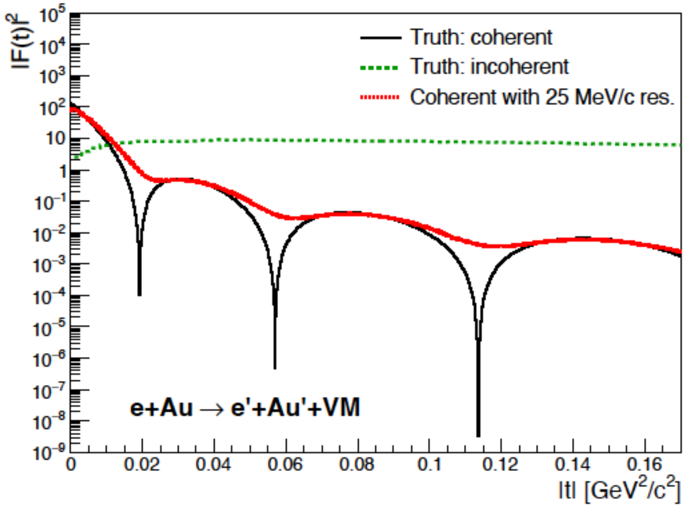

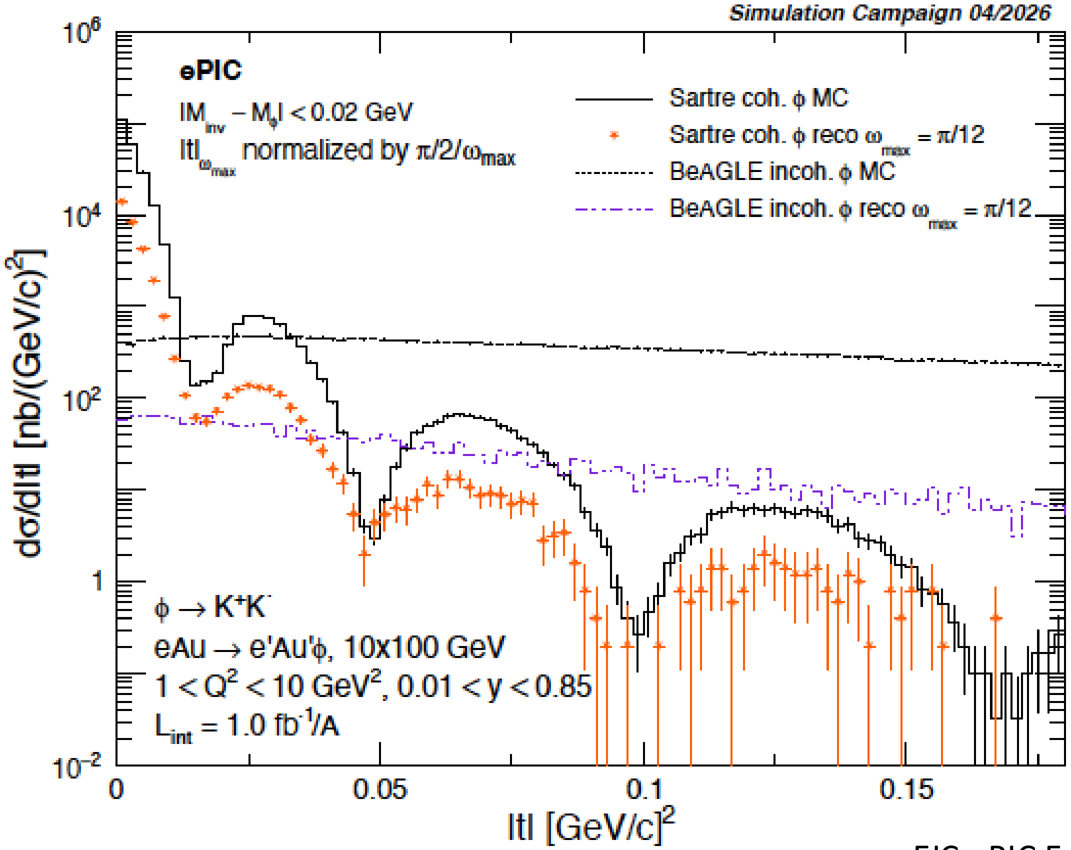

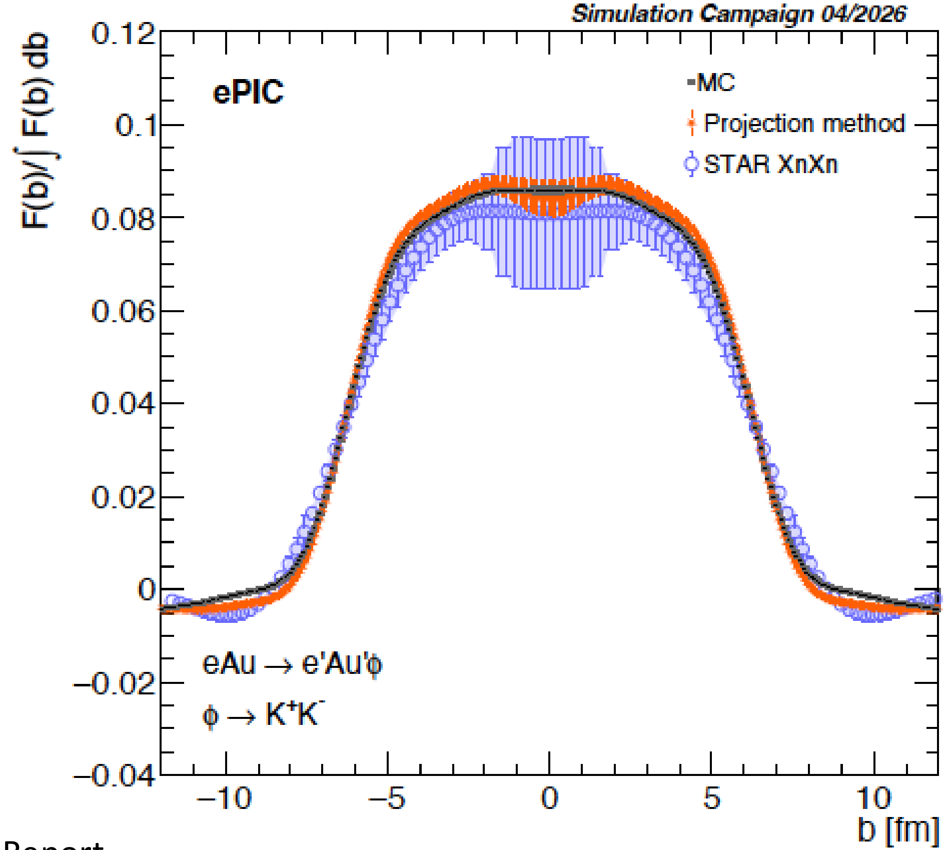

EIC ePIC Early Science Report

Baryon enhancement in p+p

ALICE, PRC 107 (2023) 064901

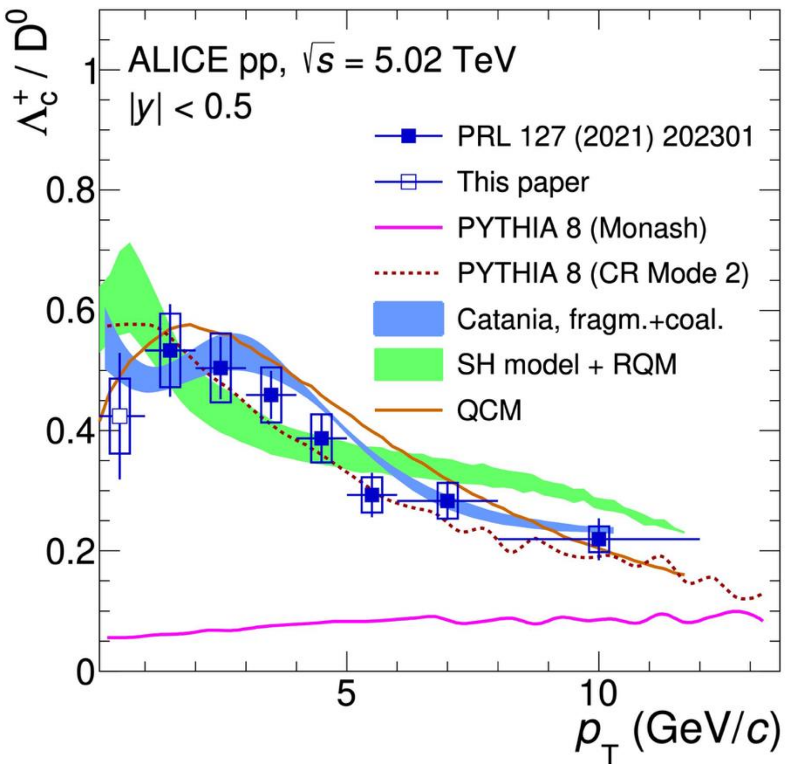

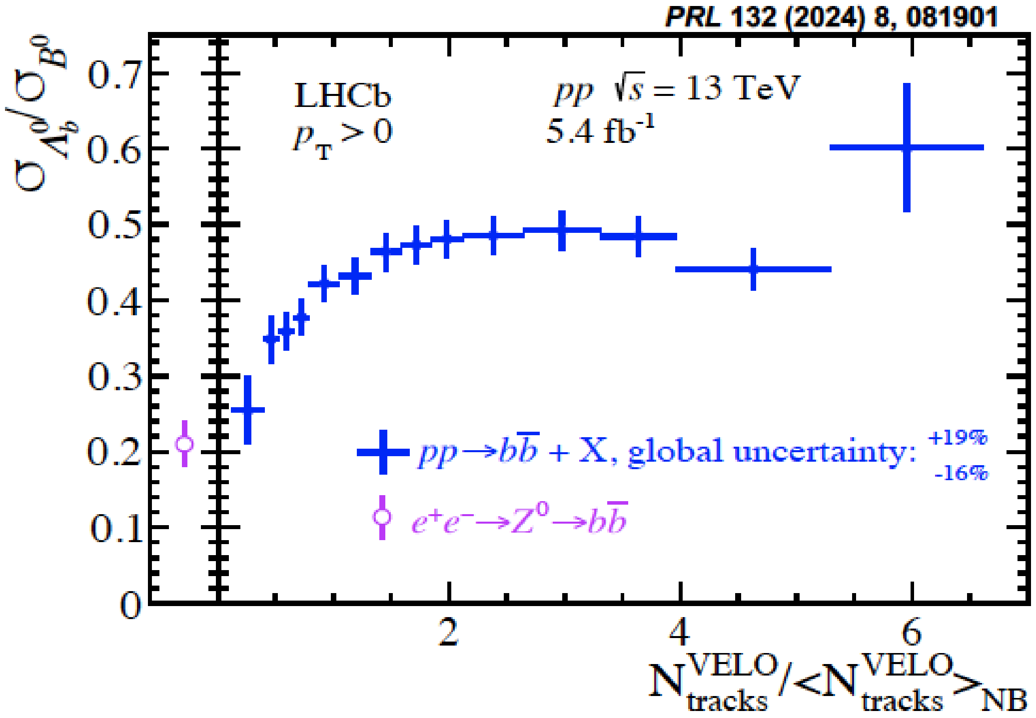

Baryon/meson ratio enhanced in p+p compared to e^+e^-

Prospects for e+p and e+A collisions

EIC ePIC Early Science Report

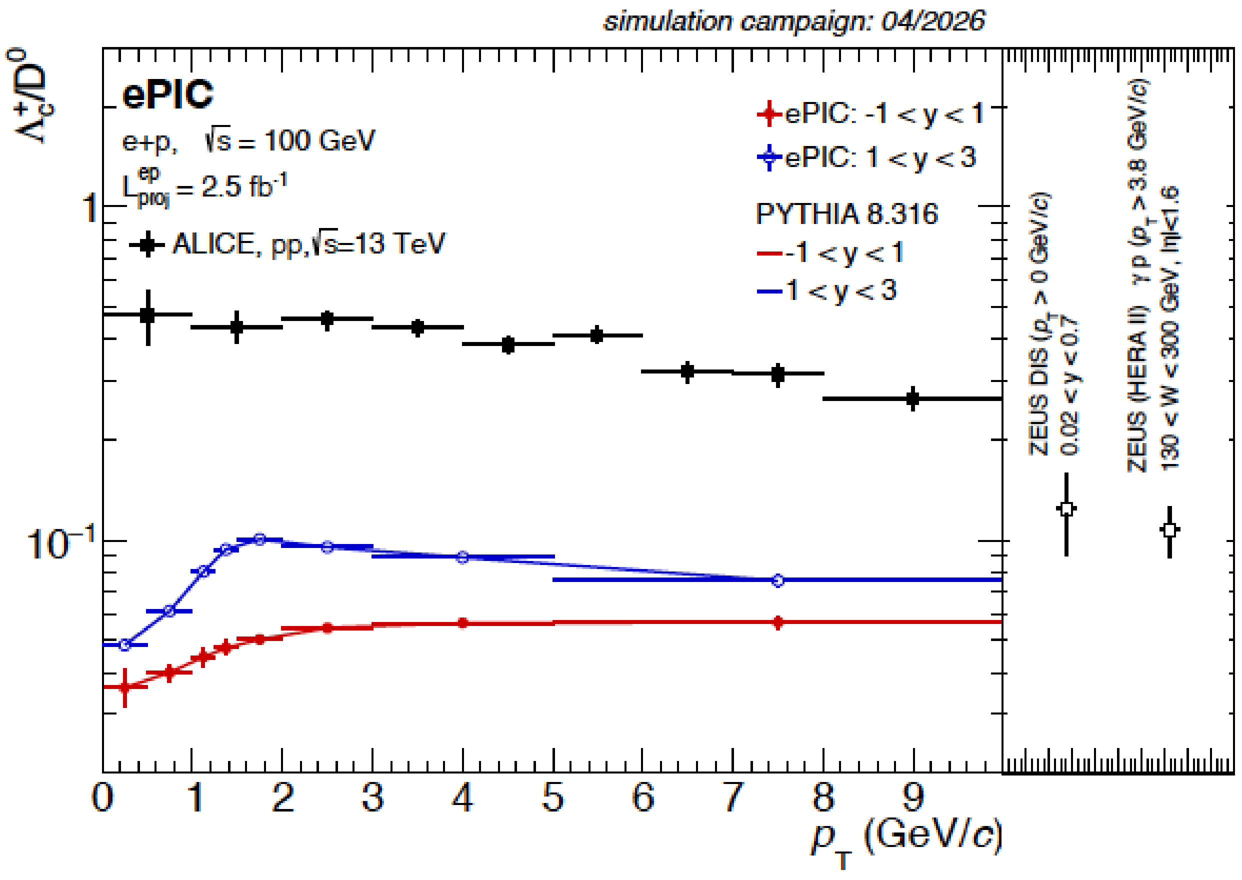

Lambda_c/D^0 ratio

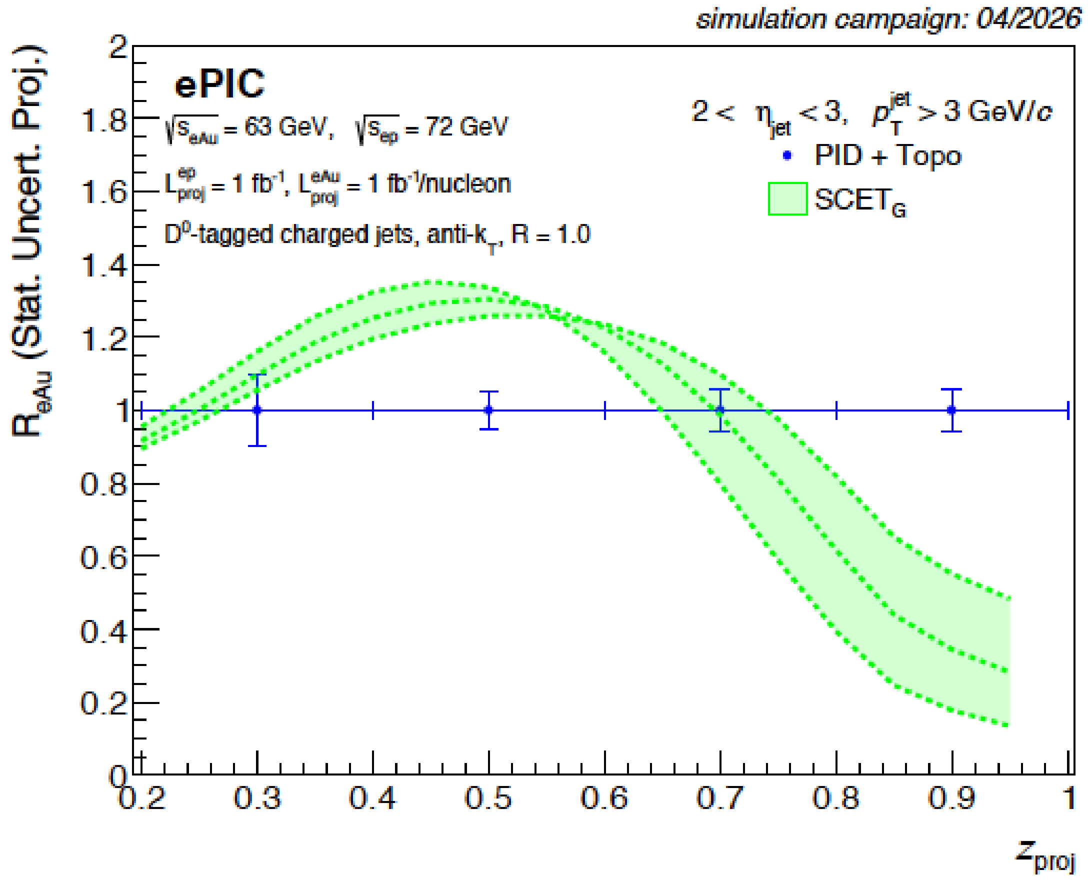

Modification to D^0 fragmentation function within charged jets

Spin correlation between quarks during QCD confinement

STAR, Nature **650** (2026) 65

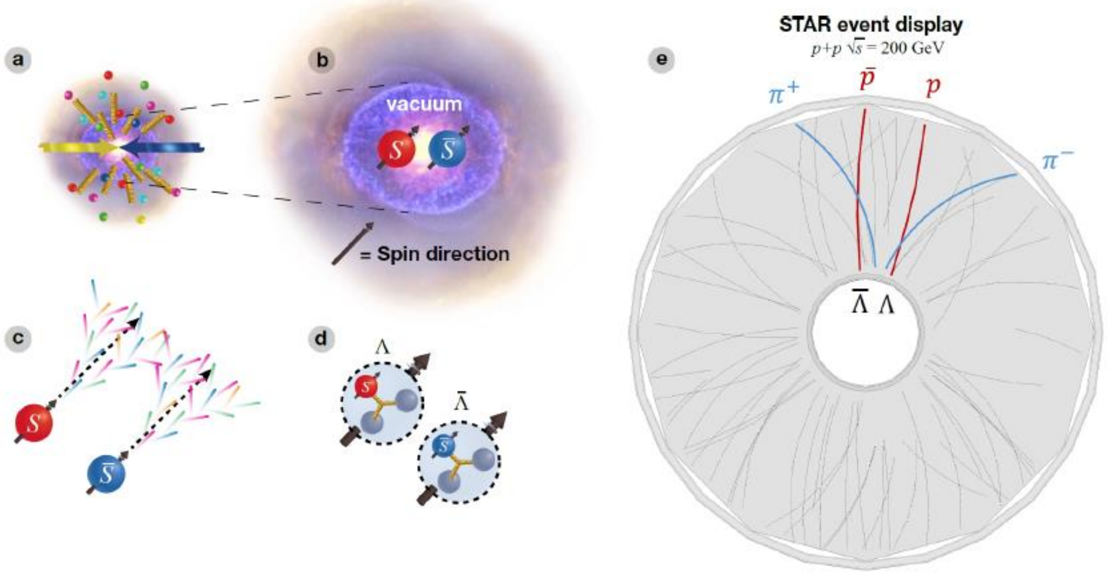

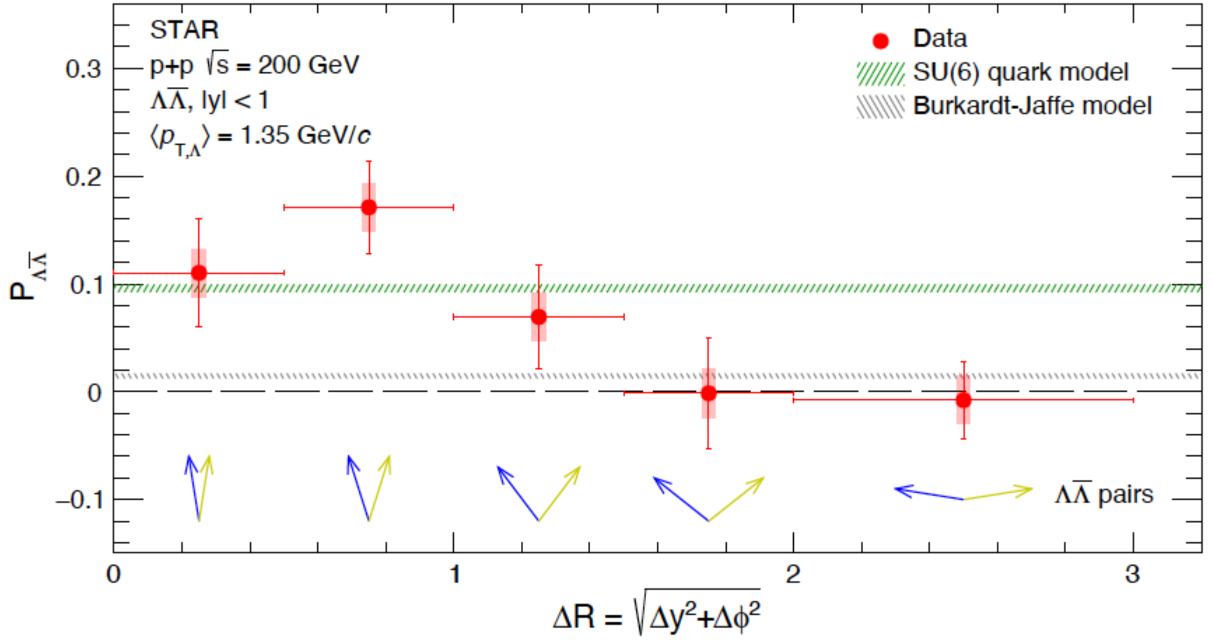

$$\frac{1}{N}\frac{dN}{d\cos\theta^*} = \frac{1}{2}[1 + \alpha_1\alpha_2 P_{\Lambda_1\Lambda_2}\cos\theta^*]$$

Spin correlation with Lambda pairs vs. pair separation

Smaller separation leads to stronger spin correlations, reaching the maximal correlation limit.

- Explore the dynamics and interplay of quark confinement and entanglement.

Summary

- **RHIC has been a discovery machine for a quarter of a century, creating and exploring many-body quantum systems with fascinating emergent phenomena. Its legacy includes:**
  - A world-leading scientific community and unique expertise
  - Innovative detector and accelerator technologies
  - Transformative scientific discoveries with broad scientific impact

- **The discovery journey continues.**

- **The EIC will open a new era of QCD exploration by using precision tomography to reveal the inner workings of many-body quantum systems and provide unprecedented insights into the many-body dynamics and emergent phenomena of QCD.**

Backup

Prospects for e+A collisions

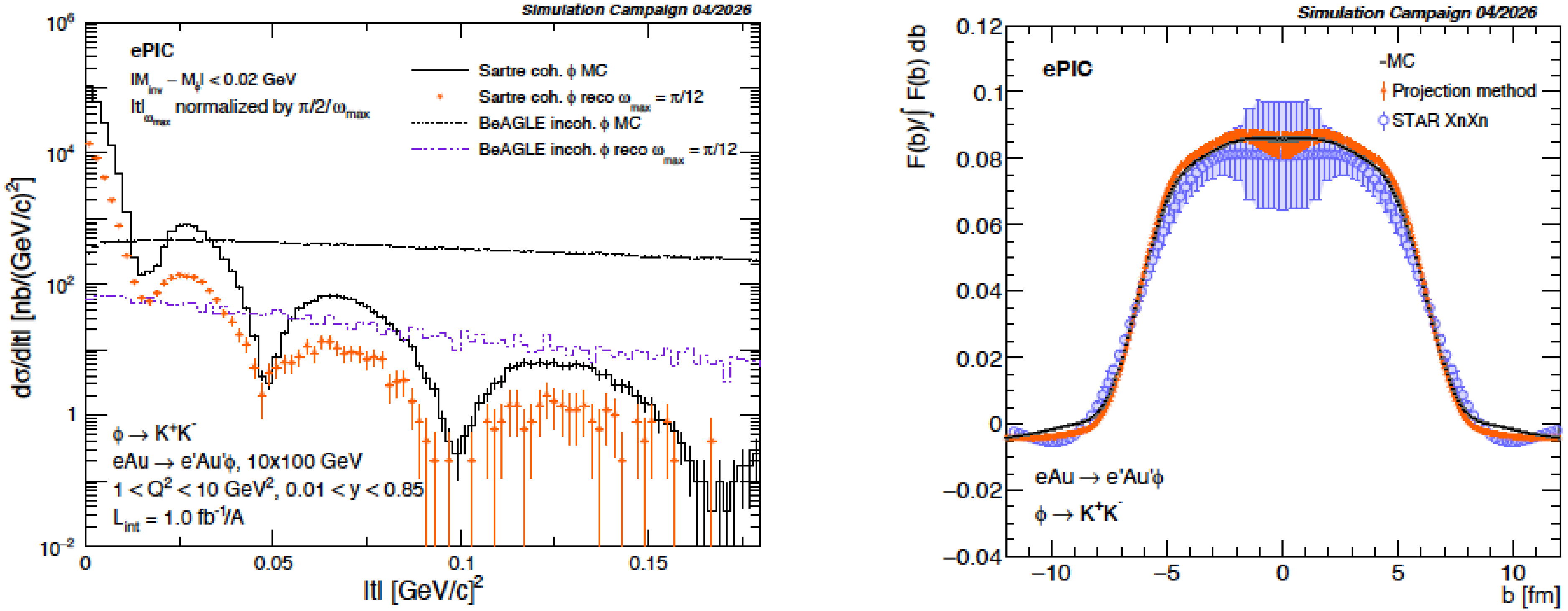

Figure 14: Left: Generated (continuous, black line) and reconstructed (orange points) $|t|$ distribution for the selection of exclusive ϕ production, with $\phi \to K^+K^-$, in $e + \mathrm{Au}$ collisions. The suppression (dotted-dashed, purple line) of the generated (dashed, black line) incoherent contribution is also shown. The reconstructed result uses the projected-$|t|$ method with a wedge selection $\omega < \omega_{\max} = \pi/12$ around the direction $\hat{n}$ normal to the electron scattering plane; the distribution is normalized by the accepted angular phase-space fraction. Right: Fourier–Bessel transform of the reconstructed $|t|$ distribution, illustrating the resulting transverse spatial gluon profile in the nucleus. The ePIC projection result is compared with the MC truth and with the STAR $XnXn$ result from coherent ρ^0 photoproduction in ultra-peripheral Au+Au collisions [176].

Prospects for e+p and e+A collisions

EIC ePIC Early Science Report

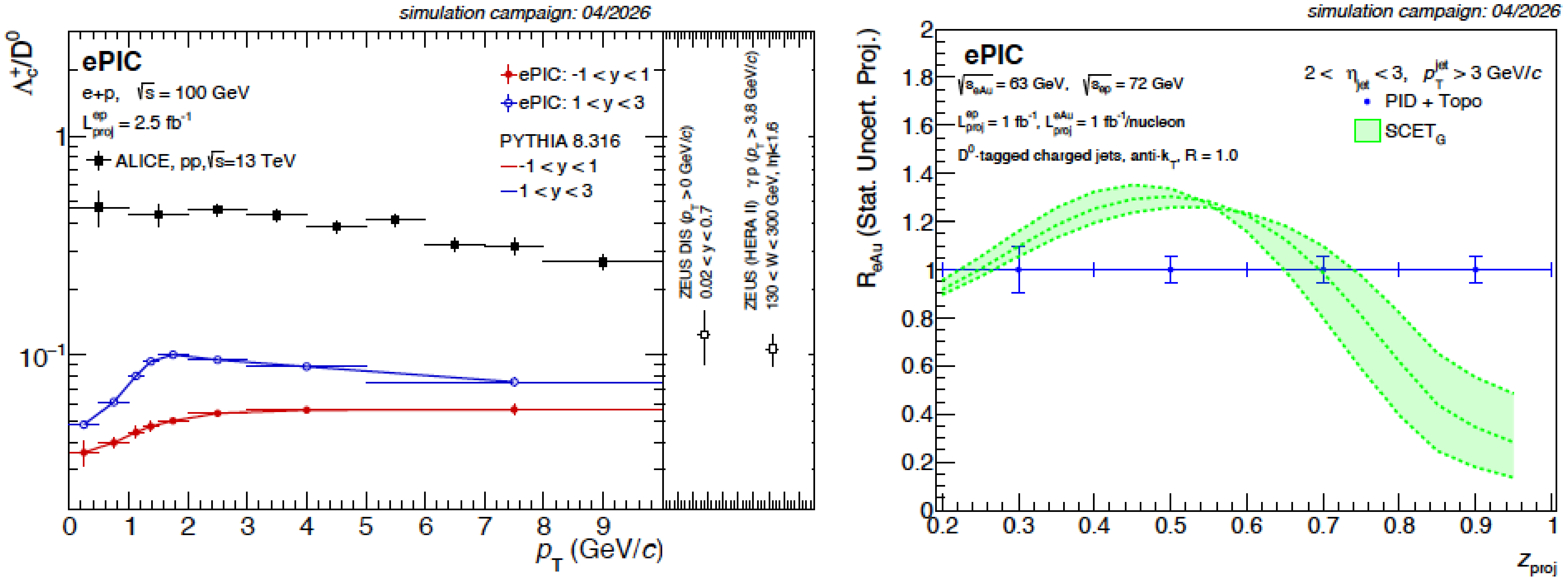

Figure 18: Left: projected inclusive Λ_c^+/D^0 ratio as a function of p_T at mid ($-1 < y < 1$) and forward ($1 < y < 3$) rapidities in 10×250 GeV^2 $e+p$ collisions. The error bars corresponds to the statistical precision for an integrated luminosity of 2.5 fb^{-1}, while the curves represent PYTHIA 8.316 predictions. The projected ePIC measurements are shown together with existing ALICE [200] and ZEUS measurements [202–204] for comparison. Right: statistical projection (blue solid markers) for the measurements of modifications to the D^0 fragmentation function within charged jets in $e+$Au collisions relative to $e+p$ collisions, in the forward region ($2 < \eta_{jet} < 3$), assuming an integrated luminosity of 1 fb^{-1}. The projection is compared with the theoretical predictions (dotted filled bands) based on soft-collinear effective theory with Glauber gluons (SCET$_G$) [207, 208].

Net-proton higher moments from BES-II

How to infer the QCD critical point

Divergence of the correlation length, dynamics slow down, Large density fluctuations

- Critical opalescence, magnetic susceptibility

Correlation length related to various moments of the distributions of conserved quantities such as net-baryon, net-charge, and net-strangeness.

Lattice calculations show that moments of the conserved charge (net-baryon, net-charge, net-strangeness) distributions are related to the susceptibilities

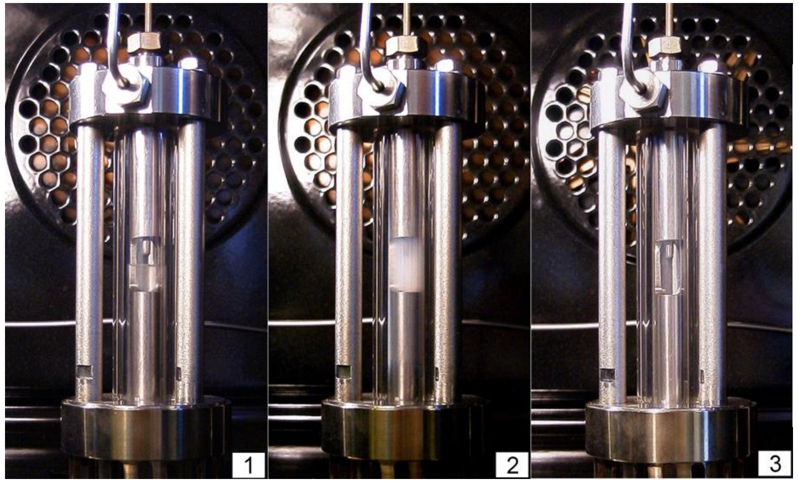

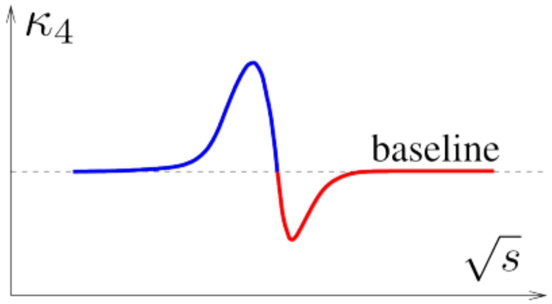

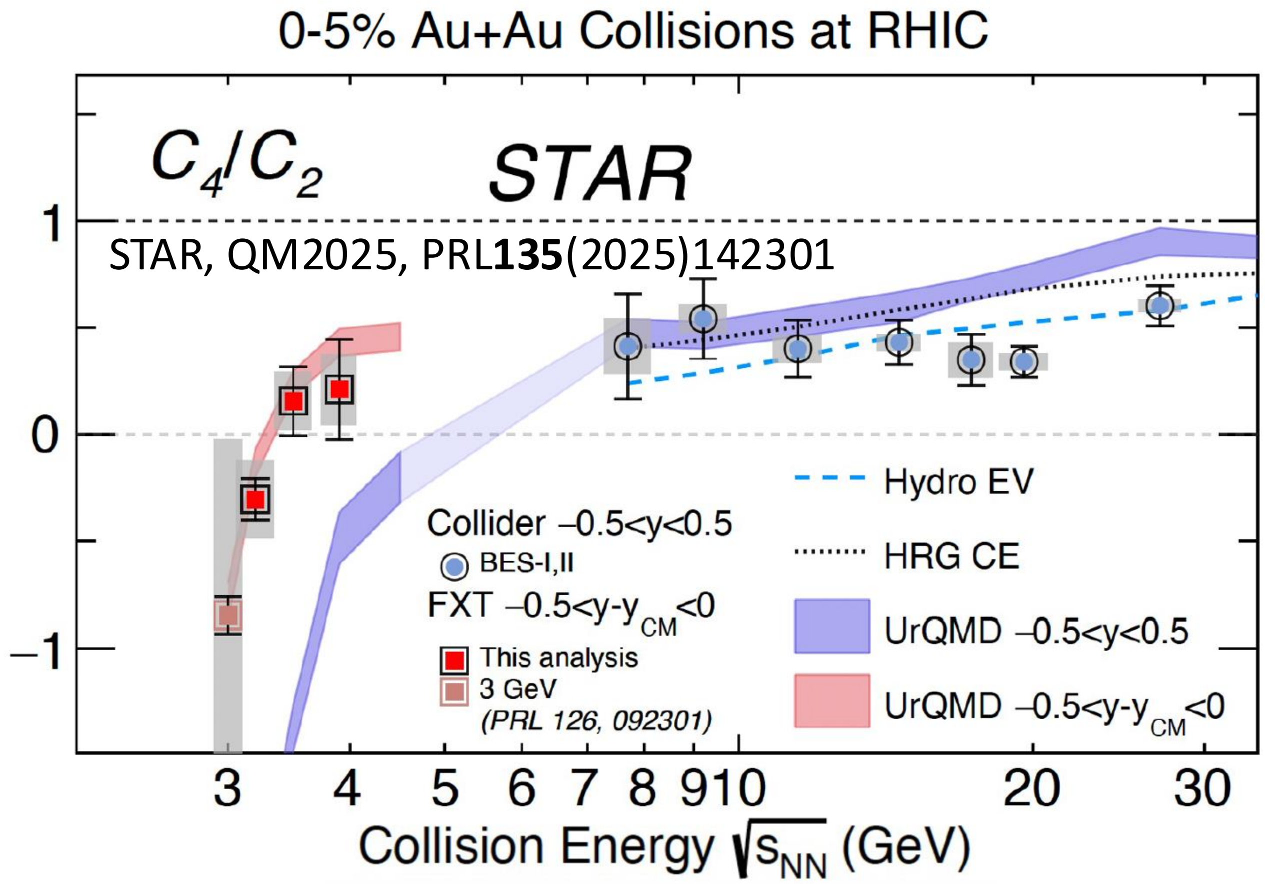

Dynamical transverse momentum fluctuations

STAR, arXiv: 2604.06434, accepted by PRL

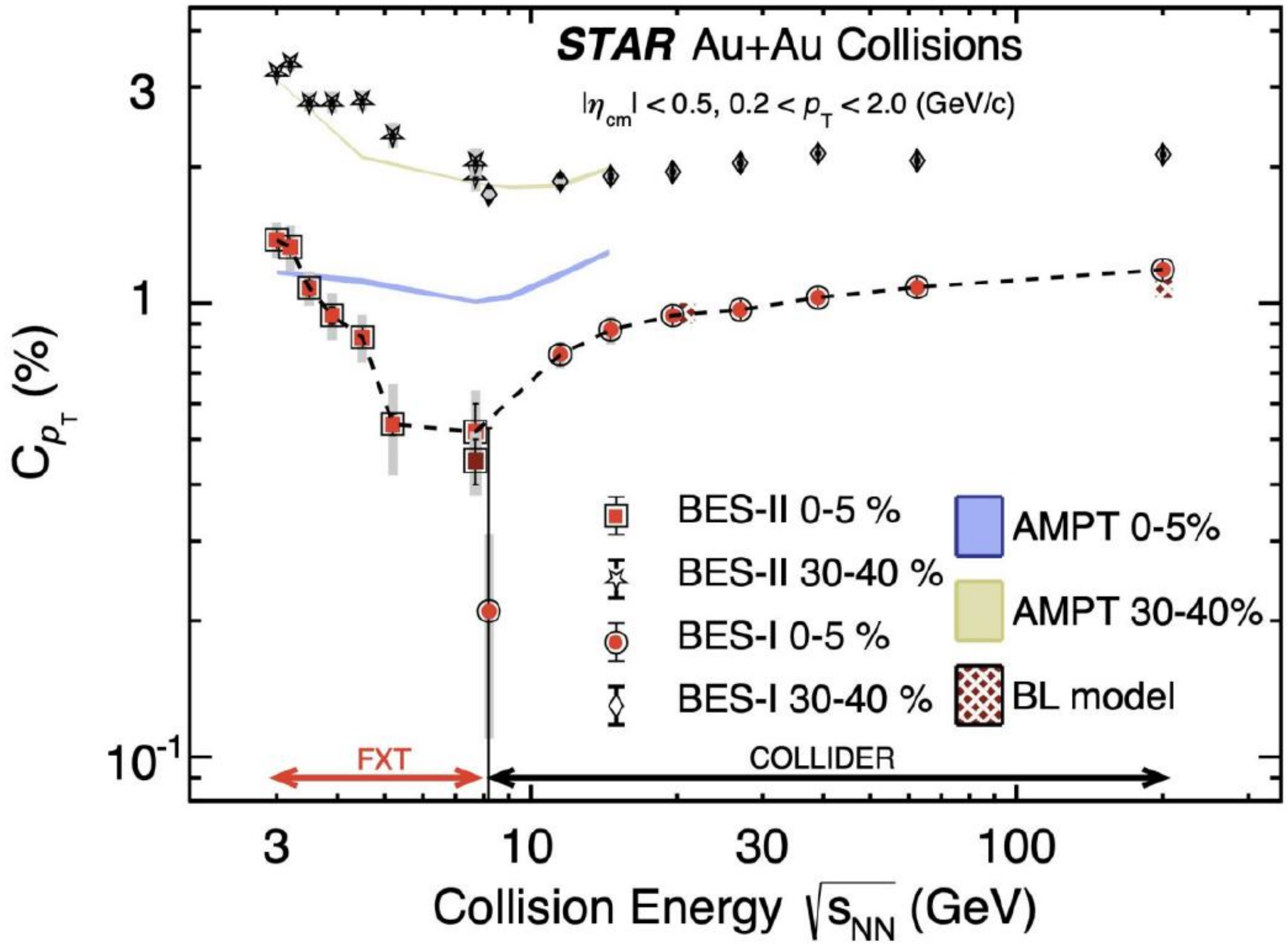

Non-monotonic energy dependence

To do:

- More comprehensive comparisons with baseline models

Longitudinal double-spin asymmetry for dijet production in pp at 200 GeV

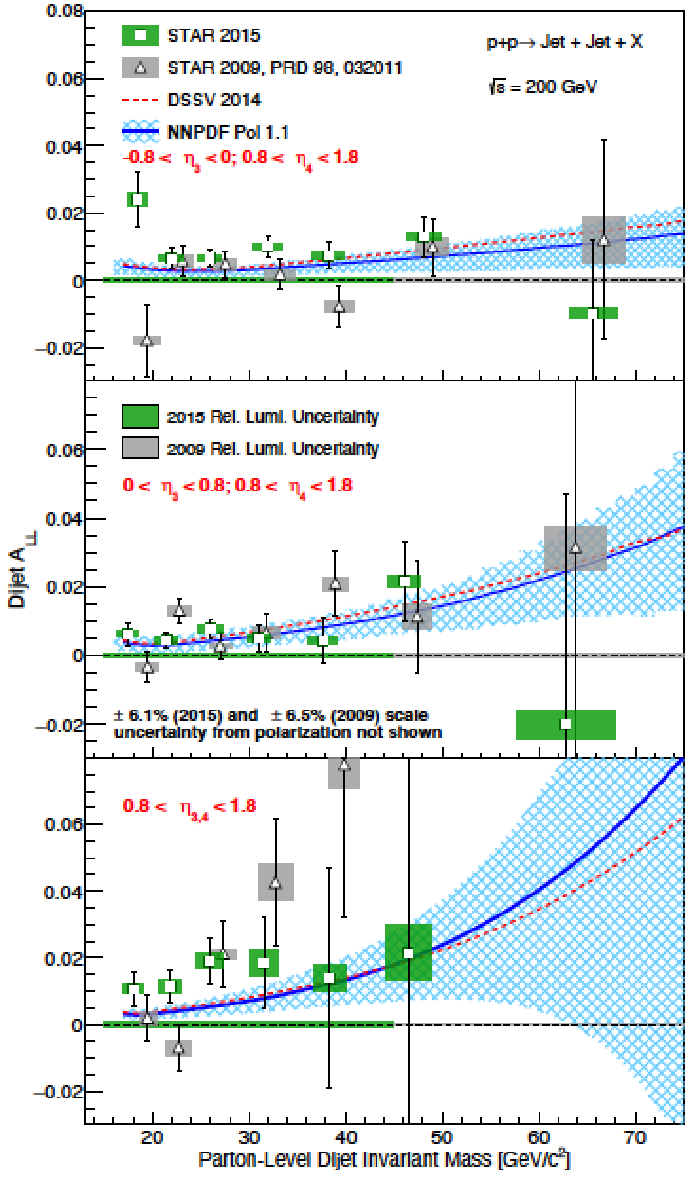

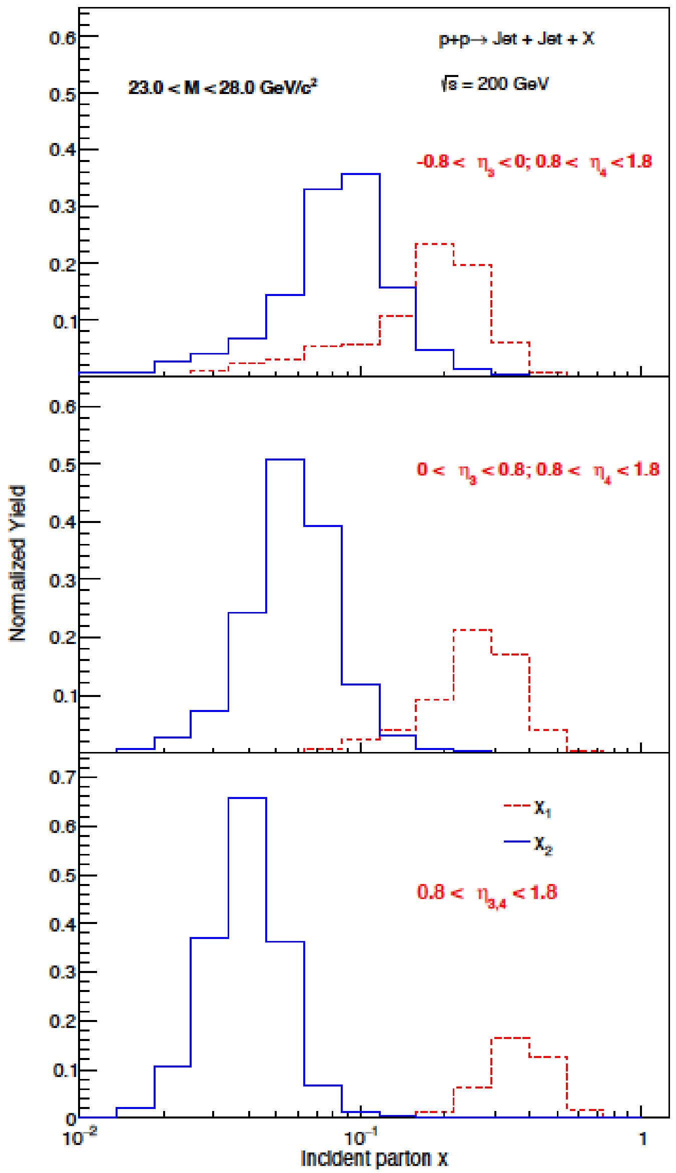

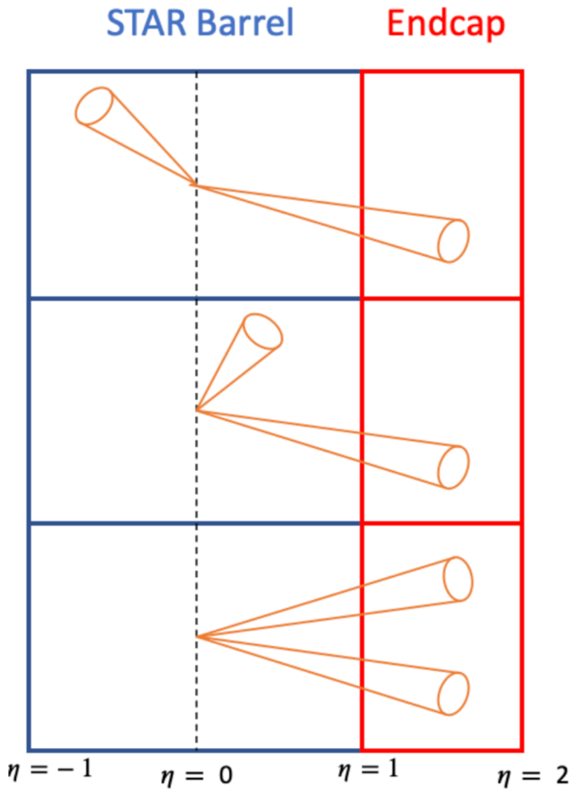

Golden probe for Δg

- Statistical uncertainty reduced by a factor of 2
- Further constrain Δg in the low x region (0.01-0.5)

STAR, arXiv: 2411.18976